Geological Society of America
Memoir 176
1990

Chapter 1

Cenozoic geometry and thermal state of the subducting slabs beneath western North America

Jeff Severinghaus and Tanya Atwater
Department of Geological Sciences, University of California, Santa Barbara, California 93106

ABSTRACT

We have reconstructed the isochron pattern of the Farallon and Vancouver plates in order to predict the thermal state and geometry of subducting slabs beneath western North America during the Cenozoic. Slabs do not last indefinitely; they warm up by conduction when bathed in the asthenosphere. As they warm up, they lose the ability to have earthquakes. Studies of modern subduction zones show that slabs become aseismic after a duration approximately equal to one-tenth their age upon subduction. Combined with a mathematical heat conduction model, these studies give us confidence that the thermal state of a slab can be characterized if we know the time since subduction and the age upon subduction. We reconstruct isochrons on subducted plates using the magnetic anomalies recorded in the Pacific plate, assuming symmetrical spreading and taking into account propagating rifts. Using the improved global plate reconstructions of Stock and Molnar (1988), we position the reconstructed plates with respect to North America to obtain maps of time since subduction and age upon subduction. The result is a series of maps of the slab geometry and approximate thermal condition at six times during the Cenozoic. With these maps we examine postulated relations between the presence and condition of the underlying slab and the occurrence of volcanism and tectonism in the overlying plate. We find that the very long flat slab proposed to have caused the Laramide Orogeny could have easily reached Colorado because of its fast average subduction rate and moderate age upon subduction, and because of the tendency for shallowly dipping slabs to last longer because they heat up more gradually while passing beneath the overriding plate. We find that the eastern edge of the proposed late Cenozoic "slab window" never existed, because of the young age of the slab. Instead, a region of effectively no slab gradually developed as early as 35 Ma, and it was farther inland than the proposed "slab window." Lacking an eastern edge, the "slab window" is better described as a "slab gap." The southern boundary of the gap is diffuse, and its location is poorly constrained, whereas the northern edge is sharp and has clear, predictable geologic manifestations.

INTRODUCTION

Subduction has dominated the Mesozoic and Cenozoic geologic history of the western United States. During much of Jurassic and Cretaceous time, geologic manifestations (e.g., Franciscan formation, Sierra Nevada batholiths, Sevier thrust belt) suggest that subduction was occurring in a rather typical steep, fast subduction zone. By contrast, the geologic records of subduction from late Cretaceous and Cenozoic times suggest some relatively unusual events, as follows. Starting in the late Cretaceous, the cessation of the Sierran magmatic belt and the occurrence, far inland, of magmatism and the Laramide Orogeny have been attributed to a shallowly dipping slab (e.g., Coney and Reynolds, 1977; Cross, 1986; Bird, 1984, 1988). A Cenozoic westward

Severinghaus, J., and Atwater, T., 1990, Cenozoic geometry and thermal state of the subducting slabs beneath western North America, *in* Wernicke, B. P., ed., Basin and Range extensional tectonics near the latitude of Las Vegas, Nevada: Boulder, Colorado, Geological Society of America Memoir 176.

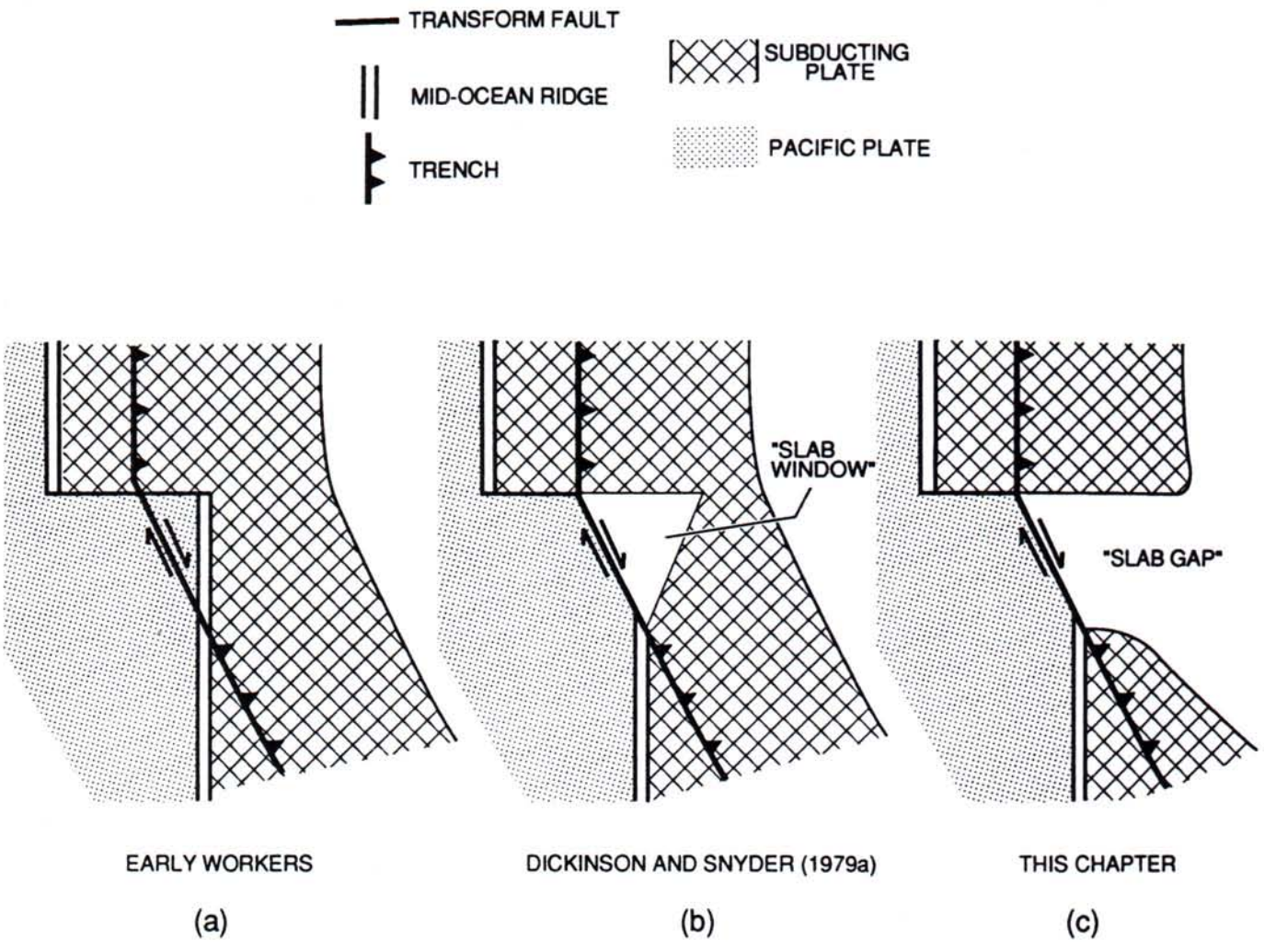

Figure 1. Schematic representation of the development of ideas on how the East Pacific Rise interacted with North America.

migration of arc magmatism seen at some latitudes has been attributed to the resteepening or disintegration of this postulated flat slab (e.g., Coney and Reynolds, 1977; Cross and Pilger, 1978).

Starting in the mid Cenozoic, the time-transgressive cessation of arc magmatism has been attributed to the replacement of the subduction system by the San Andreas boundary (e.g., Atwater, 1970; Dickinson and Snyder, 1979b). The exceptionally low seismicity and short slab length of the present-day Cascadia subduction zone has been attributed to the unusual youth of the subducting slab and the slow subduction rate (e.g., Sugi and Uyeda, 1984). All of these events and many more can be related at least partially to the slabs that were being subducted beneath North America. Thus, we undertook a project to map the geometries and thermal states of these slabs for a number of Cenozoic time steps. In this paper we present the resulting maps and discuss their implications and uncertainties.

Our primary interest concerned the mid- to late Cenozoic transition in regimes, during which the subduction system was gradually replaced by the San Andreas boundary. This occurred as the East Pacific Rise encountered the trench at the margin of North America (e.g., Atwater, 1970, 1989). The nature and geometry of this transition and its imprint on the geologic record have been the subject of a number of studies and speculations.

Some early workers supposed that the East Pacific Rise merely slipped beneath the North American plate, maintaining its precollision geometry and continuing to spread unabated as it had under the ocean (Fig. 1a). This idea is incompatible with our modern understanding of oceanic spreading systems, which except in the vicinity of hot spots, are basically passive features where asthenosphere fills in the space between diverging lithospheric plates and cools to form new lithosphere. The creation and growth of the cold oceanic lithosphere from the hot asthenosphere depends critically on the efficient removal of heat by cold seawater. If plates diverge beneath the thermal blanket of a continental plate rather than beneath seawater, the asthenosphere

filling the space will cool only extremely slowly so that no additional lithosphere will be accreted to the slabs and no coherent spreading center can be maintained.

Dickinson and Snyder (1979a) pointed out this effect and postulated that a triangular slab-free region, a "slab window," developed and grew beneath the rim of North America during the late Cenozoic (Fig. 1b). They constructed the approximate geometry of such a window for several time steps. Numerous geologic events have been attributed to the development of this slab-free region, including the cessation of arc volcanism, the evolution of the San Andreas system and its related basins, the onset of major Basin and Range extension, and the regional uplift of the Sierra Nevada and Colorado plateau (e.g., Crough and Thompson, 1977; Dickinson and Snyder, 1979a; Glazner and Supplee, 1982). Thus, the timing, geometry and nature of the slab-free region is of considerable interest to the geological community.

In this chapter, we modify and enlarge upon the slab window concept. In particular, we question the implicit assumption made by Dickinson and Snyder (1979a) that lithosphere, once formed on the sea floor, acts indefinitely as a coherent, strong slab. We assert, rather, that the duration of a slab after subduction depends critically on its age when it entered the subduction zone. In particular, young lithosphere is thin and hot, so that after subduction it will heat up and equilibrate with the asthenosphere rather quickly. In the case of the postulated slab window, the slab that would have formed its eastern edge was very young, hot, and weak when it was subducted and so would not have persisted as a coherent slab for any length of time. Indeed, it appears that this portion of the slab was fragmented before the ridge even arrived at the trench, i.e., before the window even began to form. Therefore, we conclude that a "slab gap" developed (Fig. 1c), rather than a slab window, and that it appeared earlier and farther inland than the postulated window. By a slab gap we mean a region of no slab, bordered on the north and south by coherent slabs.

Two distinct lines of evidence lead us to this conclusion. First, we present evidence from the sea-floor spreading record that the slab has been broken in this region since the early Cenozoic and that it further fragmented into several small pieces as the ridge approached the trench. The sea-floor spreading record also indicates that the larger plates to the north and south acted independently, showing that their connection had been broken. Second, we use a combination of heat conduction theory, slab seismicity observations, and plate reconstructions to model and map the thermal condition of the slabs.

Our maps of the thermal states of the slabs also contain information of interest for discussions of the Laramide flat slab scenario. Our simple thermal models show that the early Cenozoic slab was much longer and cooler than those for later times. Because of this, we conclude that the slab could have easily reached Colorado during Laramide time, contrary to the opinions of some workers that the slab would have been too hot and weak (e.g., Molnar and others, 1979). We also examine the Paleogene transition from a long, cool slab to a short, warm one as it may relate to the end of the Laramide.

We present this study in this volume to provide a larger plate tectonic context for the more local events described. Of course, we also suspect that many tectonic events of hill and mountain-range scale may ultimately be ascribed to specific plate tectonic events. Broad regions of plate interiors are primarily affected by subduction and slab-related plate events such as those examined here. In particular, the mid-Cenozoic geologic record in the region including southern Nevada and Utah, Arizona, and southeastern California should record the warming and shortening (and steepening or disintegration?) of the slab and the arrival and passage of the Mendocino slab gap edge. Although the uncertainties in the plate locations and in the continental deformation reconstructions are still too great to allow specific correlations between plate motion events and local geologic events, this study is a step in that direction.

OBSERVATIONS FROM THE SEA-FLOOR SPREADING RECORD

We made a new compilation and interpretation of the magnetic anomaly data in the North Pacific (Atwater and Severinghaus, 1989). Figure 2 shows selected isochrons from the northeast Pacific portion of these maps. These isochron patterns include three distinct indications that the subducting Farallon plate was broken throughout much of the Cenozoic.

Magnetic isochrons formed during late Cretaceous and earliest Cenozoic time are consistent with the existence of one huge, rigid Farallon plate moving to the east-northeast with respect to the Pacific plate (Rosa and Molnar, 1988). As the East Pacific Rise approached the Americas, this plate slowly narrowed, and a narrow neck developed south of the Mendocino and Pioneer fracture zones. At about 55 Ma (chron 24), the relative motion direction of the plate segment north of this neck changed to east while the segment to the south continued moving to the east-northeast with respect to the Pacific plate. Menard (1978) noted this change and named the new northern plate the Vancouver plate. Rosa and Molnar (1988) found poles of rotation for the Vancouver and Farallon plates relative to the Pacific plate, showing that these plates were indeed moving as separate bodies and that they were converging upon one another at a slow rate.

Atwater and Severinghaus (1987) and Atwater (unpublished) show that the boundary between the two plates lay midway between the Pioneer and Murray fracture zones after 45 Ma. The trace of the Pacific-Vancouver-Farallon triple junction can be seen on Figure 2 as a curving, toothlike pattern of offsets in the 45 to 30 Ma isochrons (anomalies 19–10) near 37°N, between the Pioneer and Murray fracture zones. This zigzag trace indicates that the triple junction migrated north and south many times, requiring the boundary between the Farallon and Vancouver plates to also move, which would suggest that these subducting plates were broadly sheared in the vicinity of their common plate boundary. For the purposes of this chapter, these data show that

sheared and buckled lithosphere was being delivered to the subduction zone in the slab gap region long before the gap appeared.

The fragmentation of the subducting plates became more severe abruptly at 30 Ma, halfway through anomaly 10. This change is documented by the magnetic anomaly data offshore of San Francisco, presented in Figure 3a. Our isochron interpretation, shown in Figure 3b, is modified after Lonsdale (1990). A sudden change from fast, eastward motion to slow, southeastward motion away from the Pacific plate is documented by the northeast trend and close spacing of the anomalies younger than 10.

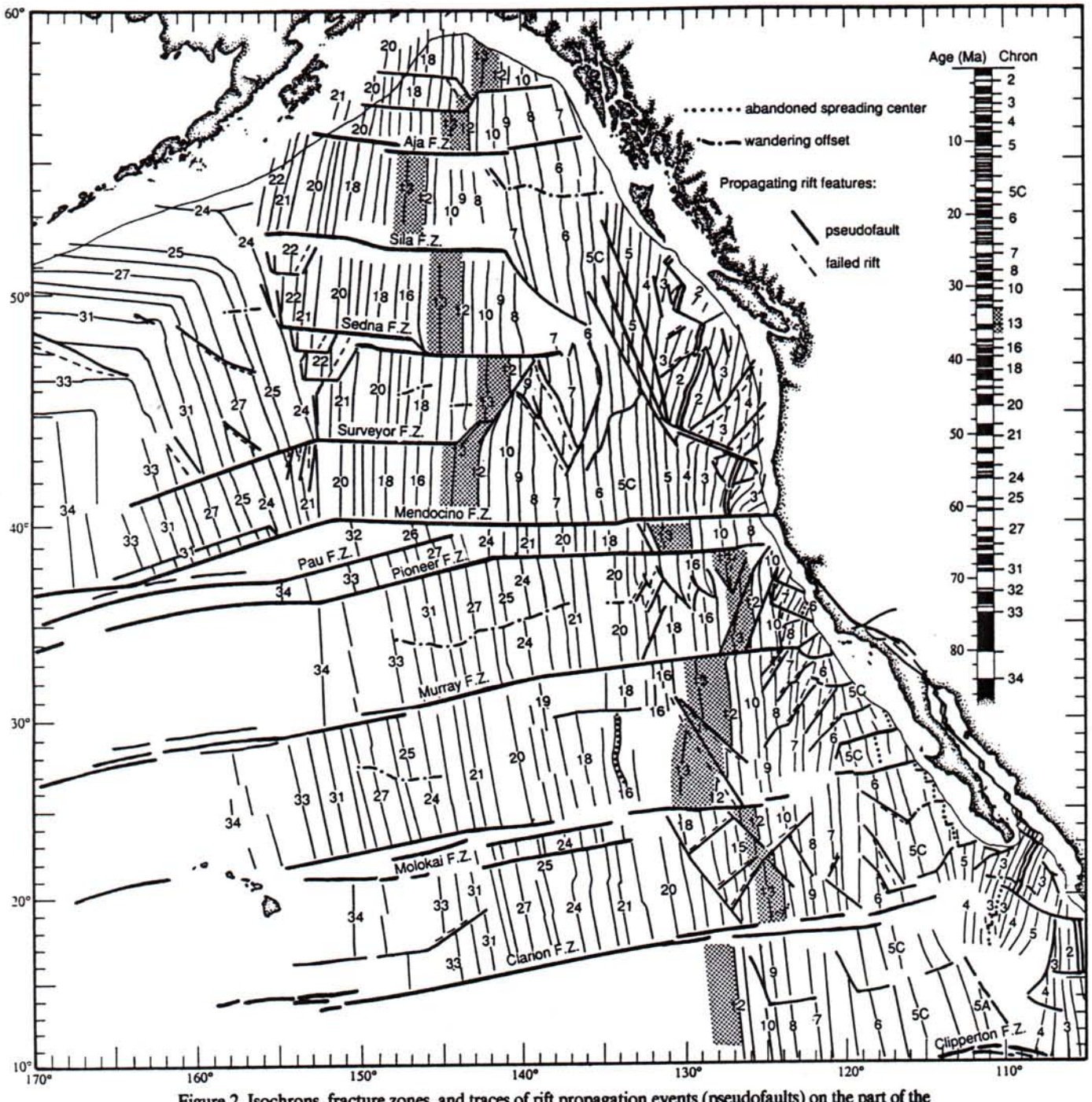

Figure 2. Isochrons, fracture zones, and traces of rift propagation events (pseudofaults) on the part of the Pacific plate used to reconstruct the Farallon and Vancouver plates, from Atwater and Severinghaus (1989). Sea floor formed at around 35 Ma has been shaded to demonstrate the early Cenozoic shape of the East Pacific rise. Magnetic chron numbers are labeled. They can be translated to dates (Ma) using the time scale shown, from Berggren and others (1985). The complete digital data set used in this study is presented in Appendix II.

The rates and directions indicate that two small plates, here called the Monterey and Arguello plates, broke free of the fast-subducting Farallon plate to the south. We note in passing that the small Monterey and Arguello plates are highly analogous to the modern situation near Vancouver Island where the Explorer plate has broken free of the Juan de Fuca plate and slowed in the last 4 m.y. (Hyndman and others, 1979).

About 19 Ma, just after anomaly 6, Pacific-Monterey spreading is interpreted to have ceased altogether, the last remnant of the Monterey plate being incorporated into the Pacific plate (Lonsdale, 1990). The defunct ridge crest is marked by dotted lines in Figures 2 and 3b near 35.5°N. It never even reached the subduction zone.

In contrast to the plate segments between the Pioneer and Murray fracture zones, the segment north of the Pioneer fracture zone did not slow as it approached the trench. Rather, this segment continued to move with the Vancouver plate away from the Pacific plate at about 120 mm/yr whole rate (Fig. 3b). It would appear that this narrow slice of young slab was firmly attached across the Mendocino fracture zone to the fast-moving plate to the north. It is the only segment that would have had the potential to develop a "slab window" with even a short-lived eastern edge,

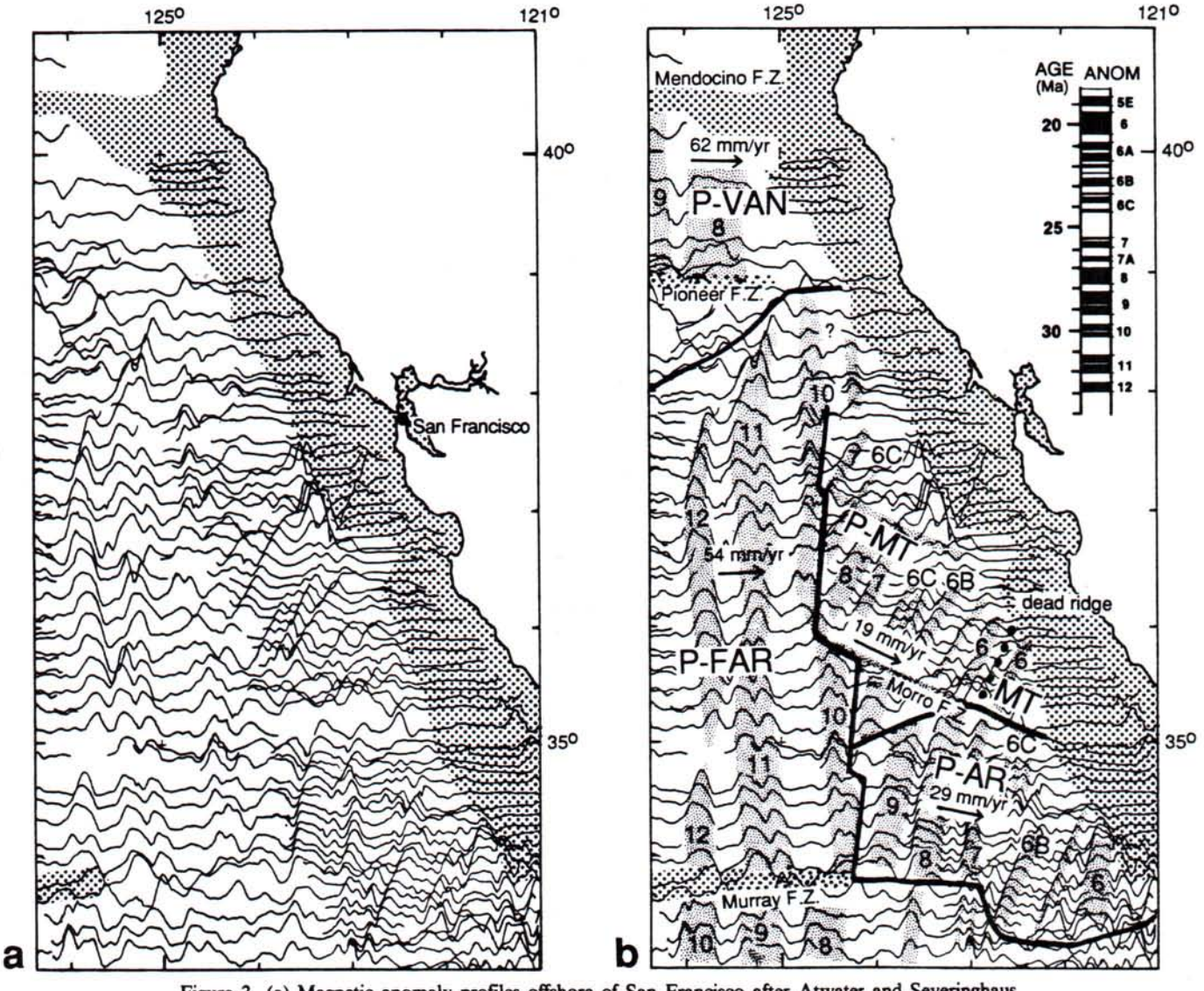

Figure 3. (a) Magnetic anomaly profiles offshore of San Francisco after Atwater and Severinghaus (1987). Systematic survey from Theberge (1971). (b) Isochron interpretation of magnetic anomalies in (a). Heavy lines delineate areas of the Pacific plate sea floor that were created by spreading between various plate pairs: P-VAN = Pacific-Vancouver spreading, P-FAR = Pacific-Farallon spreading, P-MT = Pacific-Monterey spreading, P-AR = Pacific-Arguello spreading. The Vancouver, Farallon, and Arguello plates have been entirely subducted in this area. A small fragment of the Monterey plate (MT) remains embedded in the Pacific plate southeast of the dotted line marked "dead ridge." Half-spreading rates and directions are shown by arrows. Changes in rates and trends at chron 10 (30 Ma) indicate that the slab fragmented at this time. Time scale is from Berggren and others (1985).

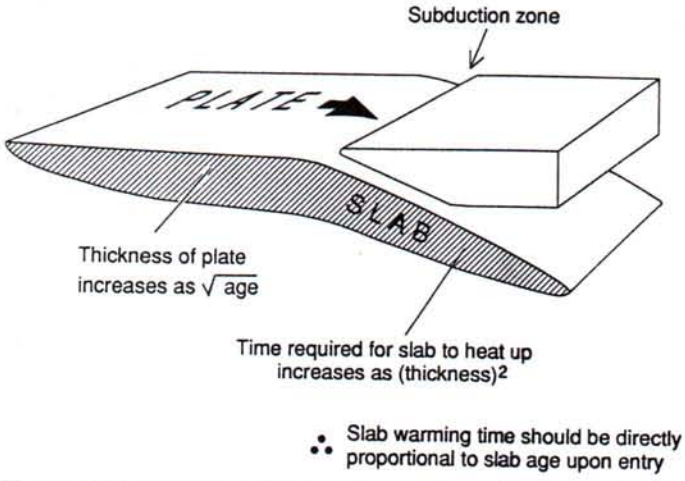

Figure 4. Results of simple heat conduction theory. Ocean floor lithosphere cools and thickens away from the mid-ocean ridge as a function of the square root of its age (Parker and Oldenburg, 1973). Subducting oceanic lithospheric warms and thins in a time proportional to its thickness squared (McKenzie, 1969, 1970). Therefore, the warming time of the slab is proportional to its age when it is subducted (see also Appendix I and Molnar and others, 1979).

since only this segment remained coherent right up to the ridge-trench encounter. This sector sharply contrasts with the one immediately to the south, in which the slab came to pieces and spreading slowed long before the ridge-trench encounter.

A third observation demonstrating the lack of coherence of the slab to the east of the window comes from descriptions of the motions of the major plates since 30 Ma. We noted above that the northern (Vancouver) and southern (Farallon) plates moved somewhat differently starting about 55 Ma, but this difference was small and their spreading directions were quite steady. Starting about 30 Ma, the Vancouver plate became quite erratic in its motions, spreading away from the Pacific about highly variable poles both to the north and south of the plate (Wilson, 1988). It is as though this plate were finally cut adrift from the larger system. The reaction of the spreading systems to this variable plate motion can be seen in the many propagating rifts that appear in the isochrons in Figure 2 starting about 30 Ma (anomaly 10).

The southern (Farallon) plate also became more erratic in its motions coming forward in time, although this is surely due in part to the Cocos-Nazca breakup at about 25 Ma and to later fragmentation of a number of additional pieces as the plate narrowed. In our slab reconstructions, we found that if we assumed that slabs remained intact indefinitely, this pivoting would require a large overlap of the two slabs and rapid sideways movement of slab through the mantle. The observed pivoting reinforces our conviction that slabs have finite lives and, in particular, that these post–30 Ma slabs did not extend far inland because of their youth.

Starting about 14 Ma, the portion of the subducting plate off Baja California broke free of the larger plate to the south and changed direction and rate, then apparently stopped spreading about 12.5 Ma (Lonsdale, 1990). Again, the spreading center stalled before it reached the subduction zone. This pattern of ridges stalling before they reach the subduction zone leads us to believe that very young, hot slabs resist subduction, due to their lack of negative buoyancy.

DESCRIBING THE THERMAL STATE OF A SLAB: THE PARAMETER *S*

Our goal is to map the approximate geometry and extent of the subducting slabs beneath North America during the Cenozoic. To do this we must devise some method to locate the point at which a slab becomes so warm that it no longer acts as a coherent body or, alternatively, the point at which it becomes incapable of inducing tectonism and volcanism in the overriding plate. In this section we define a parameter S to serve as a measure of the thermal state of a subducting slab, and we relate it to thermal models and observational data for modern slabs. We then attempt to find the value of S that corresponds to the point where, for practical purposes, the slab assimilates with the asthenosphere. Unfortunately, the latter assignment has proven to be extremely difficult. We will conclude that the assimilation point is probably about $S = 3$ or 5, but it could be as much as $S = 10$ for medium and short slabs. Fortunately, the changes in the conditions of the slabs caused by the approach of the East Pacific rise to North America are so dramatic that the implications for slab geometry are very similar no matter which of these values of S one chooses.

Mathematical models have been constructed to describe the thermal states of lithospheric plates from their creation at spreading centers to their destruction in subduction zones. As they move away from spreading centers, they cool and their thickness increases at a rate proportional to the square root of age (Parker and Oldenburg, 1973). After subduction into the asthenosphere, they heat up as the square of their thickness upon subduction (McKenzie, 1969, 1970). When these two results are combined, they predict that the time required for a slab to warm up after being subducted is approximately proportional to its age upon subduction (Molnar and others, 1979). These relations are illustrated schematically in Figure 4, and the relevant mathematical formulation and results are presented in Appendix I.

A second way to examine the thermal state of subducting slabs—an observational method—is to examine the distribution of earthquakes occurring within their cores. The dipping planes of earthquakes at most modern subduction zones are seen to have a definite lower bound, called the "seismic cutoff." The ability to store the stress required to trigger earthquakes reflects the strength of the slab, which in turn is primarily a function of its temperature (Chen and Molnar, 1983). Thus, the position of the seismic cutoff is one observable measure of the thermal state of modern subducting slabs. Molnar and others (1979) made a compilation of the lengths of seismic slabs in modern subduction zones and showed that the time required for the slabs to become aseismic is proportional to their age upon subduction, in agreement with the

mathematical models, and that it is approximately equal to one-enth their age upon subduction (Fig. 5a). In a similar study, Jarrard (1986) confirmed the linearity of the relation, although he found a somewhat greater slope, as much as 15 rather than 10, depending on various assumptions (Fig. 5b). We adopt 10 for the sake of computational simplicity.

Following these theoretical and empirical relationships, we define the parameter S. At each point on the slab, S equals the time since subduction divided by one-tenth of the age of that point at the time it was subducted. We thus arbitrarily set $S = 1$ at the seismic cutoff (it would be about $S = 0.7$ if the regression preferred by Jarrard were adopted). We then map contours of the values of S for various times in the past, given the age upon entry and the time since entry, both of which we obtain from plate reconstructions. The equation we use in our calculations is

$$S = \frac{10T}{(A-T-C)} \quad (1)$$

where A is the age of the magnetic anomaly (DNAG timescale; Berggren and others, 1985; Kent and Gradstein, 1985), T is the time since subduction, and C is the age of the particular map being constructed.

A weakness in McKenzie's (1969, 1970) mathematical description of the slab is the assumption that the top of the subducting slab is always immersed in hot asthenosphere. In fact, the tops of the slabs spend a time beneath the relatively cool overriding plate before they enter the asthenosphere. Thus, the warming of the slab will be slower at first than predicted (Jarrard, 1986), and a lag will be introduced. This lag time will be variable, depending on the dip of the slab, the amount of frictional heating generated between the plates, and the thermal structure of the overriding plate. In the observational data, the lag time manifests itself as a nonzero intercept in the correlations of Jarrard (1986) (Fig. 5b) and causes slabs with shallow dips to appear above the line in the correlation of Molnar and others (1979) (Fig. 5a).

We approximate the lag by adding 200 km to the lengths of all slabs. We chose this as an average of estimates of the lag, which range from the intercept of 303 km in Jarrard's (1986) regression (Fig. 5b) to an intercept of 100 to 150 km suggested by Figure 11 in Sugi and Uyeda (1984). The latter is a recompilation of the data of Molnar and others (1979) with a reexamination of the shortest slabs. The uncertainty introduced by this lag correction (about ±100 km) is probably not greater than the other uncertainties except in the case of the early Cenozoic, when the slab is thought to have been flat and in contact with the overriding plate as far east as the Rockies (Coney and Reynolds, 1977). In this case, 200 km is certainly an underestimate of the lag effect and, as a result, all the S values in Figure 8, below, are too high.

We note that McKenzie's (1969, 1970) mathematical formulation of slab heating used here is quite simple. A number of more complete and complex mathematical models have been developed, but we feel that these refinements would add complexity without improving our results. Most of the refinements to the mathematical formulation concern interactions with the overriding plate or the effects of phase changes, and both of these groups of effects are quite sensitive to slab dip. Our ignorance of slab paleodip and also our present inability to choose the proper S value within a factor of two, as described next, render such refinements unrealistic.

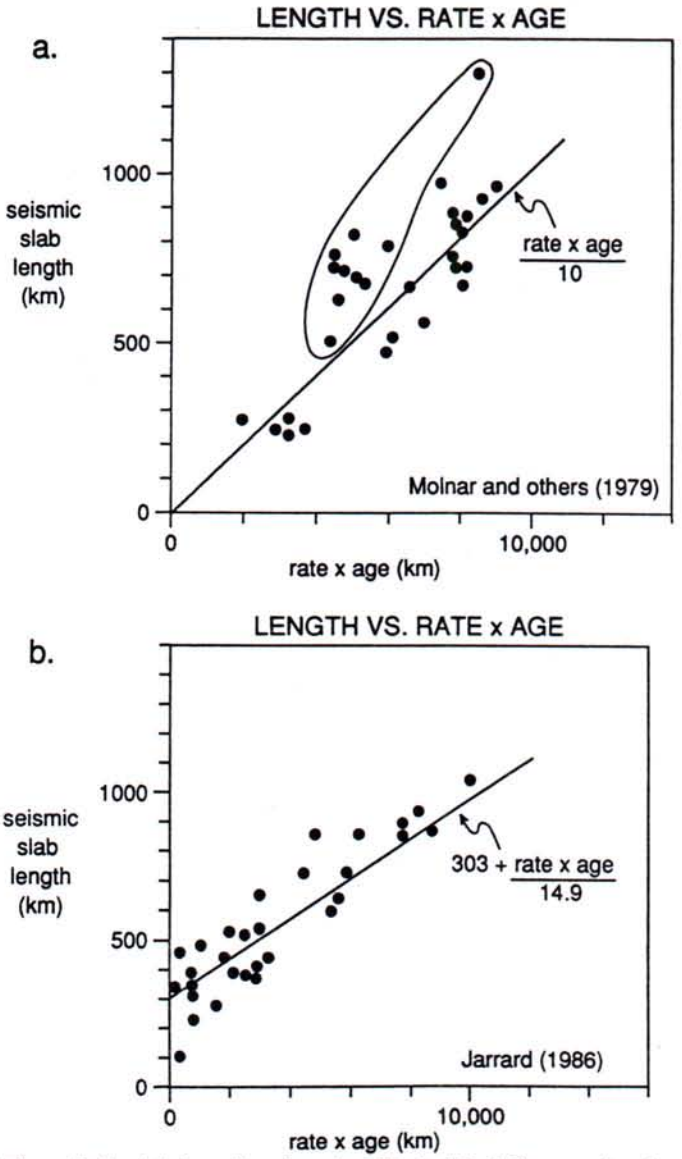

Figure 5. Empirical studies of modern Wadati-Benioff zones, showing relations among seismic slab length, subduction rate, and age on entry. (a) Plot of down-dip length of modern seismic zones versus convergence rate times age of the subducting lithosphere at the trench, from Molnar and others (1979). Slabs with dip less than 30° are circled. The tendency for these low-dip slabs to be several hundred kilometers longer than predicted (i.e., to lie above the line) can be explained if slabs warm up more slowly while passing beneath the overriding lithosphere. (b) Same relation with some new data and slightly different methods: Age is an estimate of the slab age at the seismic cutoff extrapolated from the age gradient near the trench, and back-arc spreading is not included in convergence rates, from Jarrard (1986). Line is the author's preferred regression of selected points.

HOW LONG DO SLABS LAST AFTER BEING SUBDUCTED?

Our interest in this chapter is to map the ancient extent of coherent subducting slabs beneath North America. We emphasize that the seismic cutoff, $S = 1$, is merely one measure of the thermal state of the slab and that the slab certainly can last beyond that point. Unfortunately, how much farther a slab persists beyond the seismic cutoff is not well known, even for present-day subduction zones.

Slab duration can be conceptualized in several different ways; it can be a measure of (1) how long slabs remain capable of inducing arc volcanism and tectonism, (2) how long they are detectable as a mantle seismic velocity anomaly (high velocity suggests the presence of cold material), or (3) how long they last as a coherent body before they disaggregate. Although the first question is the most interesting from a geological standpoint, the latter two are more approachable. We examine the latter two questions and presume that slabs will become incapable of inducing tectonism and volcanism well before they disaggregate or become seismically undetectable.

Modern old, cold lithosphere subducting at fast rates often extends as a seismic slab to a length of 1,000 km or more and a depth of nearly 680 km in the earth. Seismic velocity anomalies are reported beneath some of these slabs, extending a few hundred kilometers farther down (Creager and Jordan, 1986). These anomalous regions can be interpreted to be the aseismic extensions of the slabs into the lower mantle and, as such, would suggest that the slab is still present and detectable to perhaps $S = 1.5$. However, these long, deep slabs may not be relevant to our study since they encounter the 680-km discontinuity, a horizon in the mantle believed to represent a large increase in viscosity (Hager, 1986) and hence a profound impediment to the passage of slabs, if they pass through at all.

More relevant modern examples are those subduction zones with slower rates and/or younger lithosphere. Relatively well-studied examples are the medium- and short-length slabs at the Aleutian and Cascadia subduction zones, respectively. Analysis of seismic P and PcP wave velocity anomalies beneath the Aleutian arc indicates that the slab extends at least down to 600 km depth, with some indications that it may continue to 1,000 km (Boyd and Creager, 1987, and personal communication, 1988). The seismic cutoff occurs here at about 250 to 300 km, so we conclude that the slab still exists and is detectable as a velocity anomaly to about $S = 3$ to 5.

The Cascadia subduction zone is the best studied example of a modern short slab, but unfortunately, it presents some important difficulties that limit its usefulness to our study. The subducting lithosphere is young and the subduction rate is slow, so that the calculated S contours occur relatively near to the trench, predicting a short slab. However, in this case, the lag in heating during contact with the overriding plate introduces a very large uncertainty, as large as the length of the slab itself. Furthermore, the subduction is mostly aseismic, so that the location of $S = 1$ is not easily established in the field. The Cascade volcanoes do demonstrate that arc volcanism can occur over aseismic slabs, but because of the uncertainty in the lag correction we cannot determine the value of S beneath the arc. The one part of this slab that may be helpful to us is the section passing beneath Puget Sound. Here some earthquakes do occur in a dipping plane, reaching to about 100 km depth (Weaver and Baker, 1988). A region of slightly high seismic velocity extends downward with about 65° dip from that point and is detectable to about 400 km (Michaelson and Weaver, 1986; Rasmussen and others, 1987). If we place $S = 1$ at the last earthquakes and adjust our calculated S values accordingly, we calculate a tenuous S value of about 7 for the slab at 400 km.

These observations of the various slab lengths, although they are quite variable, do give us independent confirmation that the slabs extend beyond the seismic zones, beyond $S = 1$. Furthermore, since seismic velocities are quite sensitive to temperature variations, the fact that the slabs are not presently detectable beyond about $S = 5$ or 7 leads us to believe that they are approaching mantle temperatures by that time.

Another way to predict slab duration is to study the results of mathematical thermal models and try to estimate the temperature at which the slab would be too hot to continue to act coherently. The oceanic lithosphere is often described as a quasi-rigid plate underlain by a viscous "thermal boundary layer" (Parsons and McKenzie, 1978). The temperature at the boundary between these two regimes is generally taken to be about 0.75 of the asthenosphere temperatures, or about 975°C (Parsons and McKenzie, 1978). We may, by analogy, suppose that when the cold core of the slab warms beyond this temperature it will no longer hold together as a coherent body.

Olivine flow laws derived from laboratory studies (Goetze, 1978), when extrapolated to strain rates appropriate to this problem (3×10^{-15} s^{-1}), predict that olivine begins to flow significantly in this temperature range (975°C) and hence are in general agreement with the temperature assumed for the thermal boundary layer (Chen and Molnar, 1983). By way of comparison, the temperature at the seismic cutoff is estimated to be significantly lower, between 600 and 800°C (Molnar and others, 1979; Wortel, 1982).

As seen in Appendix I, Figure A3, slab core temperatures of 975°C occur at about $S = 3$ to 4. A strong slab probably does not persist beyond about this point. The core of the slab reaches a temperature of 0.97 of asthenosphere temperature at $S = 10$, i.e., it is nearly indistinguishable from the asthenosphere.

Because of the great uncertainty in actual slab duration, we show contours as far as $S = 10$, but we do not in fact believe that strong slabs extend beyond about $S = 3$. Fortunately, the changes in slab thermal state through the Cenozoic are so striking that the particular choice of S value for slab assimilation makes little difference to the conclusions.

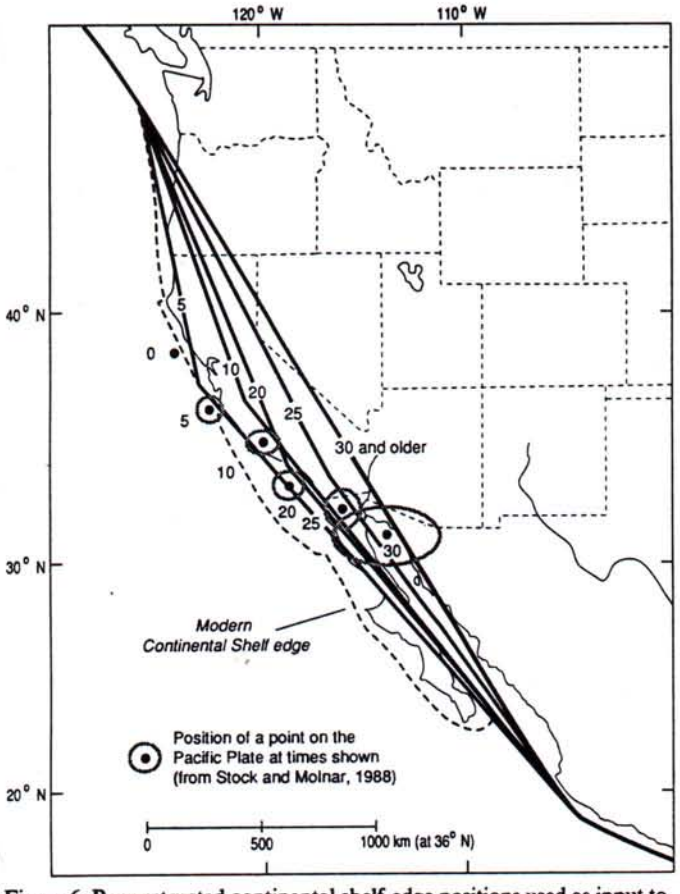

Figure 6. Reconstructed continental shelf-edge positions used as input to the thermal model. These were generated by assuming that the coast of North America distended as if pinned to the Pacific plate at the Mendocino fracture zone and with pivot points at the mouth of the Columbia River and Gulf of California. Pacific plate positions and uncertainties with respect to a fixed North America are shown by a sea-floor test point, calculated from global circuits by Stock and Molnar (1988) for the times listed (times in Ma). This distension is generally consistent with other reconstructions (e.g., Frei, 1986) and is assumed to reflect the combined effects of Basin-and-Range extension and deformation in California.

RECONSTRUCTIONS OF THE EDGE OF NORTH AMERICA

In order to map the thermal state of slabs, we must know the approximate location of the edge of North America through the Cenozoic. In particular, we need to account for changes in trench position due to Basin-and-Range extension and strike-slip deformation. To approximate this, we make the assumption that a test point on the Pacific plate just south of the Pioneer fracture zone was the same distance from the continental shelf edge at 30 Ma that it is today (see Fig. 6 for location of this point). We then allow the coastline to distend, coming forward in time, as if it were two chords pinned to stable North America at the mouth of the Columbia River and the mouth of the Gulf of California, and pinned to the Pacific plate near the Mendocino Triple Junction (Fig. 6). In essence, we use the global circuit to predict the timing and amount of continental deformation.

One justification for the assumption that the test point was no farther from the continent at 30 Ma than it is today is that the global plate circuit, if correct, requires 340 ± 200 km of Basin-and-Range extension along an azimuth of S60°W or 500 ± 250 km along N70°W (Stock and Molnar, 1988). This is already near the upper limit permitted by geologic constraints (Wernicke and others, 1988). If the trench were some distance farther east of the test point than it is today, even more Basin-and-Range extension must have occurred, which we find geologically unpalatable.

Although obviously an oversimplification, this reconstruction of the continental edge is compatible with reconstructions based on a combination of geologic constraints from the Basin and Range province and paleomagnetic reconstructions that combine rigid body rotation of the Oregon and Washington Coast Ranges with no rotation of the Sierra Nevada (Frei, 1986). Note that this approach results, coincidentally, in a straight coastline before the ridge-trench encounter at 30 Ma.

We recognize that this reconstruction is an approximation and note that errors in our assumed trench positions will introduce errors in our calculated slab thermal conditions. The location of the trench determines the ridge-trench distance and, therefore, the amount of time the lithosphere can cool before entering the trench. However, this uncertainty is small compared to our uncertainty in assigning the lag time due to the overriding plate, so we do not treat it further.

CONSTRUCTION OF MAPS OF THE SLAB THERMAL STATE

Figure 7 shows an example, at 20 Ma, of the steps in the method used to map the inferred thermal state of the slab. Using an interactive graphics computer, we found rotation poles for many short steps in the spreading history of the magnetic anomalies on the Pacific plate. We then used these rotations and their combinations to reconstruct isochrons on the Farallon and Vancouver plates, assuming symmetrical spreading and taking into account the propagating rifts (Fig. 7a). Next, we positioned these plates with respect to North America using the Pacific–North America global circuit of Stock and Molnar (1988) and using a deformed rim of North America, as described in the previous section. From these reconstructions we created a map of time since subduction (Fig. 7b) and a map of age upon entry (Fig. 7c). The ratio of these two parameters, multiplied by ten, yielded the final product, a map of the inferred thermal state of the slabs beneath North America 20 m.y. ago, presented as contours of S in Figure 11, below.

The positions of the contours of S, mapped in this way and presented in Figures 8 through 13, are subject to some significant uncertainties. Since some of these uncertainties are quantifiable and some are quite subjective, we have not attempted a rigorous analysis of the total uncertainties. Rather, we show components

of the uncertainties that can be quantified and have simply described the rest. On our maps we include the global circuit error ellipses of Stock and Molnar for Pacific–North America positions and a subjective slab-length error resulting from this global circuit uncertainty plus our estimate of Pacific-Farallon uncertainties. In Figure 8 alone, the slab-length error includes all additional sources of error, since these are especially large for this particular reconstruction.

THERMAL STATE OF THE SLAB THROUGH TIME

Figures 8 through 13 show the inferred thermal state of the slabs from 50 Ma through the present. Contours for $S = 1, 2, 3, 5$, and 10 are shown. Note that we have not corrected the locations of the contours for slab dip. For a 45° slab dip, the contours should be moved coastward about 30 percent. Since the dip is suspected to be highly variable, sometimes very shallow, and since the importance of the contours lies not in their absolute locations but rather in their striking order-of-magnitude variations through time, we chose not to include this factor.

State boundaries are shown in Figures 8 through 13 for reference, with Basin and Range extension and strike-slip deformation approximately removed back to 30 Ma. Total deformation is made to fit our assumption for the position of the trench, while the distribution of deformation is guided by geologic constraints.

50-Ma reconstruction

Figure 8 shows contours of S in the slab at 50 Ma, toward the end of the Laramide Orogeny. We have little information about the age of the crust formed during the Cretaceous Quiet Period, between magnetic anomalies 34 (84 Ma) and M0 (118 Ma). This reconstruction was made assuming steady symmetrical spreading during the Quiet Period on the ridge segment south of the Murray fracture zone. Crustal ages were interpolated linearly between 84 and 118 Ma on all ridge segments. Also, this reconstruction was made on a flat Earth, unlike the other reconstructions, which were done on a sphere.

The large uncertainty introduced by these assumptions turns out to have little effect on our overall conclusions. The slab age was probably between 40 and 60 m.y. upon entry, giving a seismic cutoff ($S = 1$) between 4 and 6 m.y. after entry. Using the average subduction rate of 120 ± 20 mm/yr between 70 and 50 Ma (Stock and Molnar, 1988) and adding the 200 km lag, the seismic slab length would have been between 600 and 1100 km. Although this length is uncertain by a factor of two, it is much longer than those calculated for the later Cenozoic.

Note that the $S = 2$ contour is near Denver, Colorado, meaning that the slab has been subducted about twice as long as necessary to become aseismic. Note also that if the slab were flat and in direct contact with the overlying lithosphere of the North

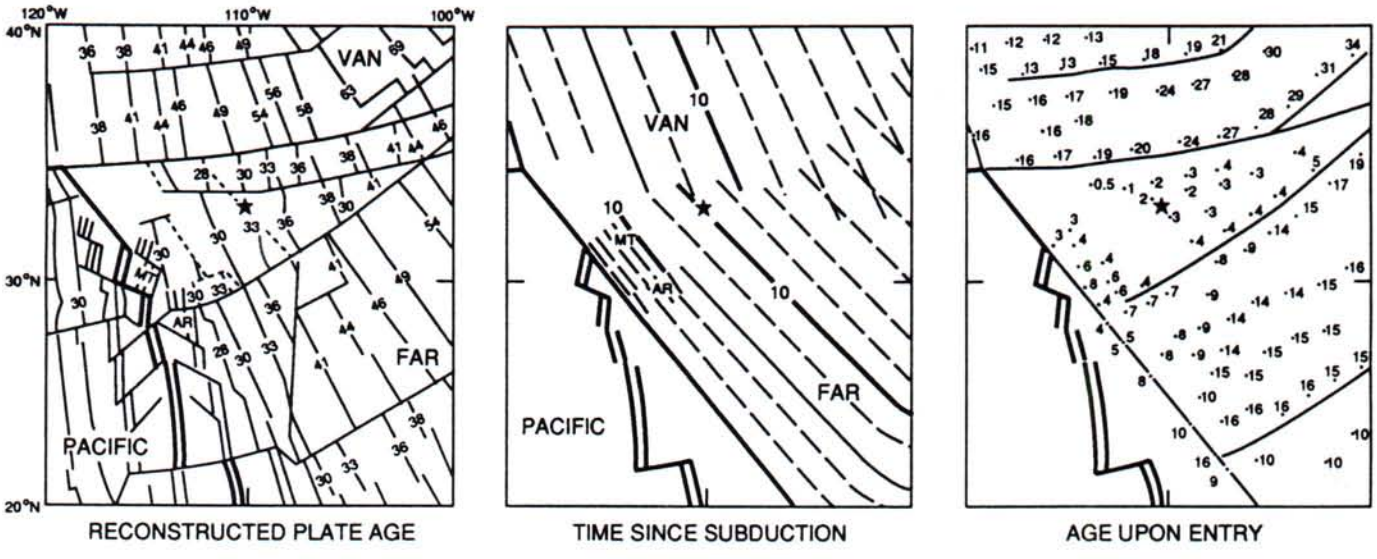

Figure 7. Examples from reconstruction for 20 Ma, showing method used to construct contours of S in the slab. (a) Map of reconstructed isochrons on Farallon (FAR), Vancouver (VAN), Monterey (MT), and Arguello (AR) plates. Ages (Ma) of magnetic anomalies from DNAG timescale (Berggren and others, 1985). (b) Map of time since subduction, showing trench positions on the slabs at intervals of 2 m.y. Solid lines are independent determinations; dashed lines are interpolations. (c) Map of age upon entry, made by subtracting values in (b) and reconstruction age (20 Ma) from (a). S values are calculated by dividing values in (b) by those in (c), times 10. For example, the star is located on the reconstructed anomaly 12, age 33 Ma. It has been subducted for 10 m.y. at the time of this 20-Ma reconstruction, so it was 3 m.y. old when subducted. Thus, its predicted thermal state is $S = 33$, meaning that it has been subducted 33 times longer than necessary to become aseismic.

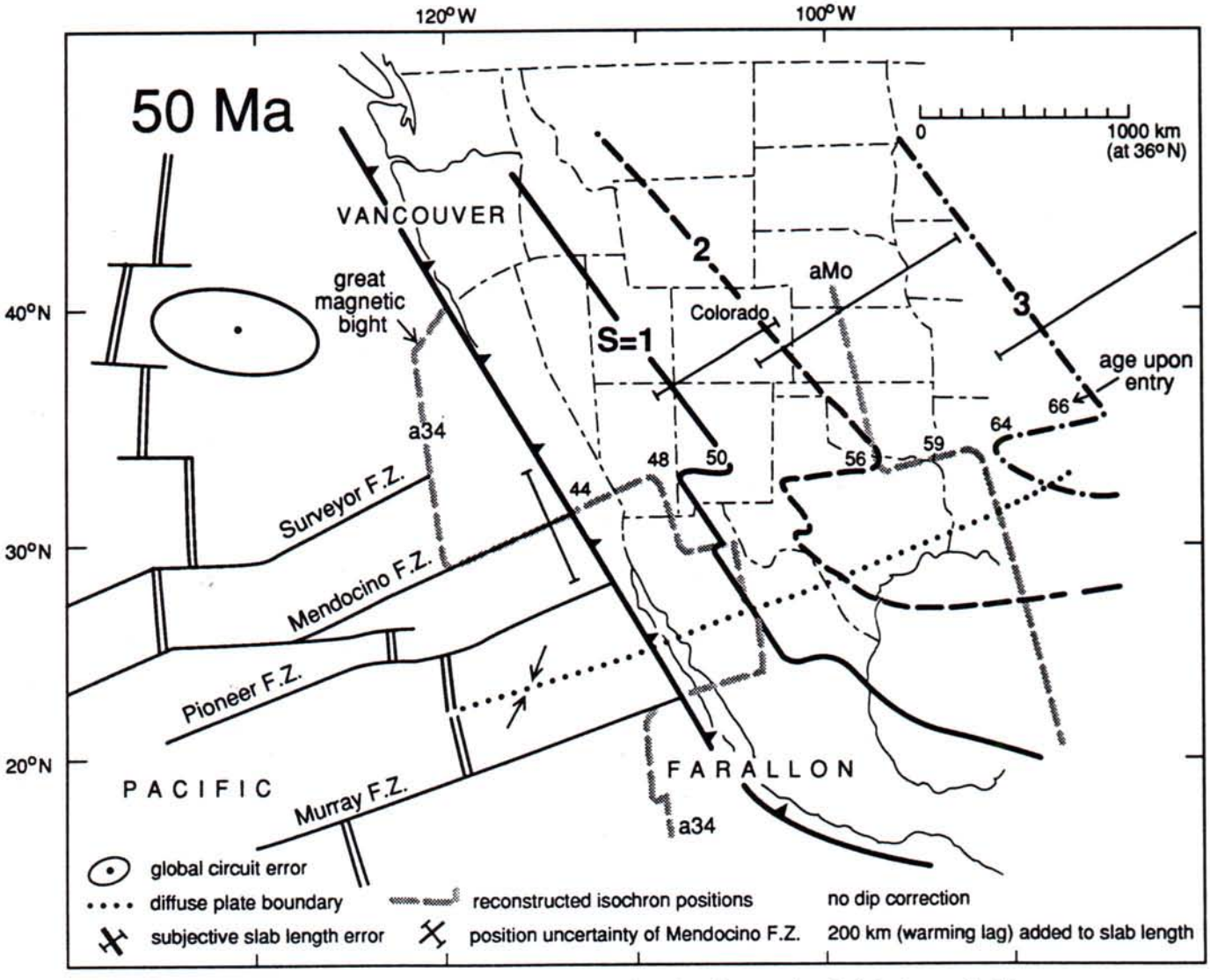

Figure 8. Inferred slab thermal state at 50 Ma, showing the existence of a relatively long, cold slab during the Laramide Orogeny. Large, heavy numbers indicate values of S; light numbers show age on entry (Ma). Pacific plate position with respect to North America with uncertainty (ellipse) is taken from the global circuit reconstruction of Stock and Molnar (1988). Gray lines show positions of the reconstructed aM0 and a34 isochrons. Because of ambiguities in the spreading history during the Cretaceous quiet period, a34 is the eastern limit of well-known crustal age. Dotted line shows approximate position of the Vancouver-Farallon plate boundary, and arrows on this boundary show relative motion across it. We conclude that the flat slab hypothesis cannot be ruled out on the basis that the slab would have been too young and hot to reach beneath Colorado; in fact, it could have easily extended this far.

American plate, as is often asserted, it would have been heated mostly from below, so that the equation for S seriously underestimates the seismic slab length.

We portray our best estimate of the summed uncertainties in the "subjective slab length error" bars shown in Figure 8. Because of the many uncertainties in this particular reconstruction, the actual values of S are poorly known. The primary value lies in its striking contrast to the much shorter slabs of the later Cenozoic.

35-Ma Reconstruction

Figure 9 shows contours of S in the slab at 35 Ma. The slab has significantly shortened everywhere. If the early Cenozoic flat slab scenario is adopted, this shortening of the slab is probably recorded by the mid-Cenozoic westward sweep of magmatism reported in many areas (e.g., Coney and Reynolds, 1977; Cross and Pilger, 1978; Cross, 1986). The nearly simultaneous matur-

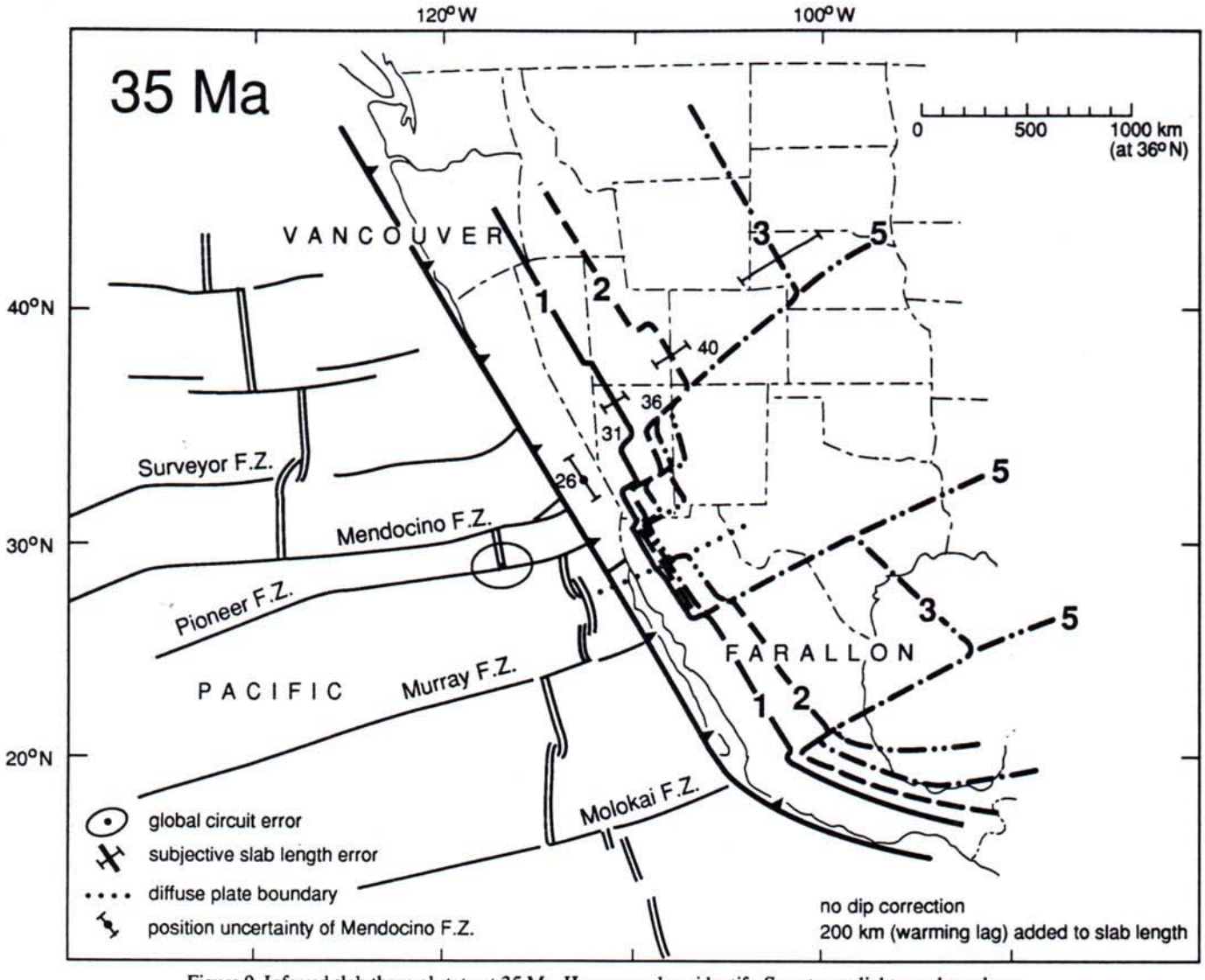

Figure 9. Inferred slab thermal state at 35 Ma. Heavy numbers identify S contours; light numbers show age on entry (Ma). S contours approach the trench from the east as the ridge approaches the trench from the west, creating a symmetrical hourglass shape. Except for the short slabs near the coast, the slab sector between the Pioneer and Murray fracture zones is already hot and weak enough that it is best described as a "slab gap."

ing of a long portion of the slab suggests that this shortening event may not necessarily have taken place as an orderly steepening and "roll back" of the slab, as is often imagined, but rather that it disintegrated piecemeal over a large region, as depicted in Figure 10 of Cross and Pilger (1978), for example.

At 35 Ma the slab is already extremely short between the Pioneer and Murray fracture zones, the future site of the slab-free region, reaching $S = 5$ and 10 within a few hundred kilometers of the coast. We infer that except for the near-coast region where the young slab persists, this section of the slab has been reassimilated into the asthenosphere, leaving a "slab gap" between northern Mexico and New Mexico. Note that this is 15 to 20 m.y. earlier than the time when the "slab window" as proposed by Dickinson and Snyder (1979a) would have grown to significant size; subduction is still occurring all along the western margin of North America at this time.

30-Ma Reconstruction

Figure 10 shows contours of S in the slab at 30 Ma. At this time, the slab segment between the Murray and Pioneer fracture zones broke free of the Farallon plate to the south. Presumably, it had become so thin and warm that it was no longer strong enough to remain rigidly attached to and moving with the Farallon plate, and its own slab no longer supplied enough negative buoyancy to maintain fast subduction.

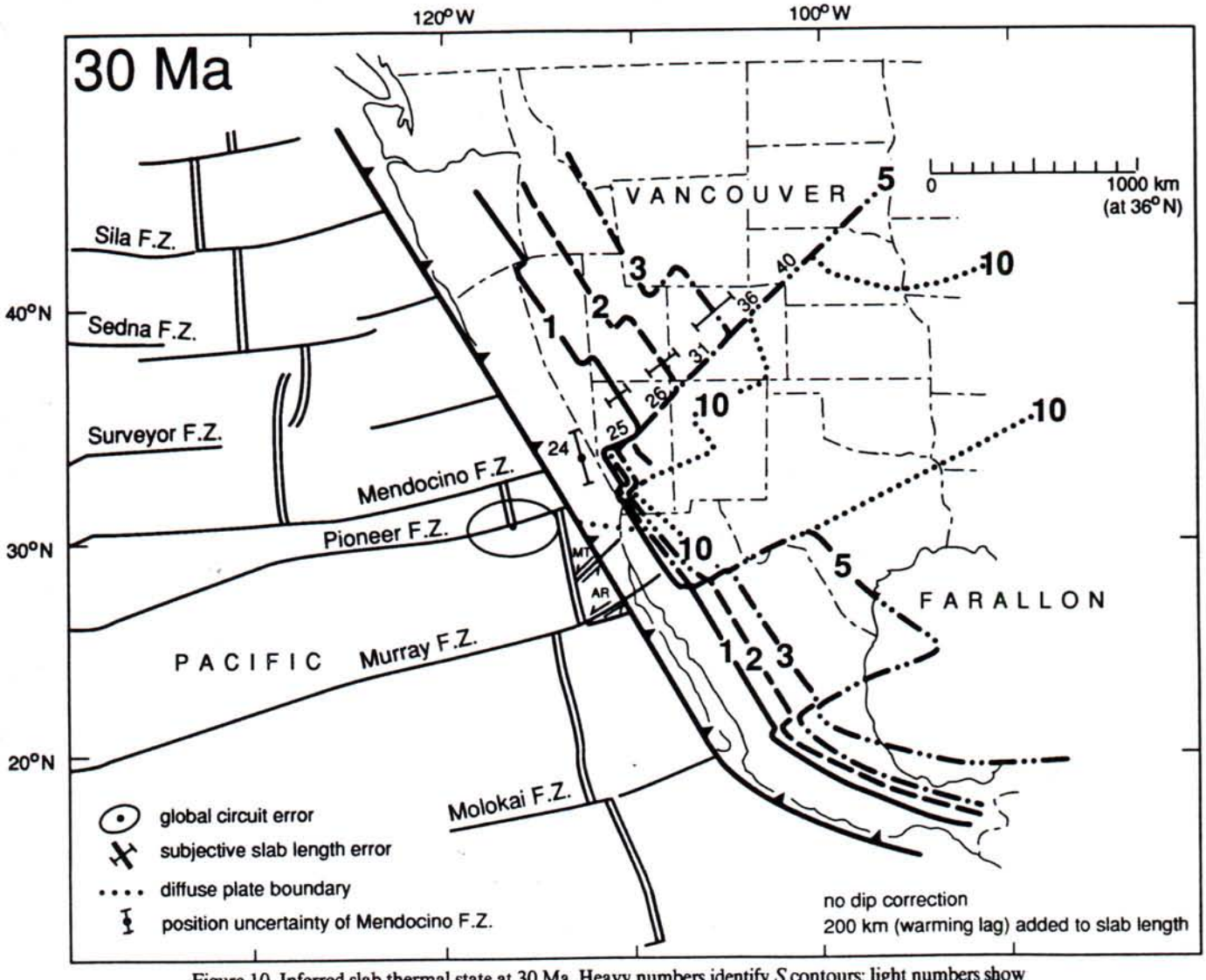

Figure 10. Inferred slab thermal state at 30 Ma. Heavy numbers identify *S* contours; light numbers show age on entry (Ma). Almost all of the slab between the Pioneer and Murray fracture zones shows values of *S* greater than 10. The Farallon Slab broke at this time, forming the Monterey (MT) and Arguello (AR) plates. Small plate boundaries are drawn assuming they are strike-slip boundaries, by analogy to the present-day Nootka fault separating the Explorer and Juan de Fuca plates.

The strike slip faults drawn between the newly formed Monterey and Arguello plates and the Farallon plate are speculative. We use the analogy, mentioned above, of the modern Explorer plate. This small plate broke free of its parental Juan de Fuca plate along the Nootka fault, a strike-slip fault oriented in the direction of relative plate motion (Hyndman and others, 1979). Thus we draw our new plate boundaries parallel to the directions of relative motion between the various plates.

It is interesting to speculate on the geometry of the subterranean breaks in the slab that led to the birth of the Arguello and Monterey plates. Although the exact geometry cannot be resolved, we argue that the strike-slip faults mentioned above would be likely to extend down through the slab to the deep, plastic regions of this very short slab. Thus, our bias is that the entire slabs of these plates slowed with the plates, with primarily strike-slip breaks between them.

Another alternative is that the small plates may have separated from their slabs along trench-parallel breaks of extensional nature. Relatively buoyant basalt undergoes a phase change to much denser eclogite at depths estimated from 40 to 80 km (Ringwood and Green, 1966; Pennington, 1983). Eclogite is more dense than ordinary mantle and is thought to be an important factor in the slab-pull force to which plate motion is attributed. Because buoyant basalt resists subduction while eclogite drives it, the basalt-eclogite transition would be a likely place for a slab to break free of the plate it is pulling. If such a break

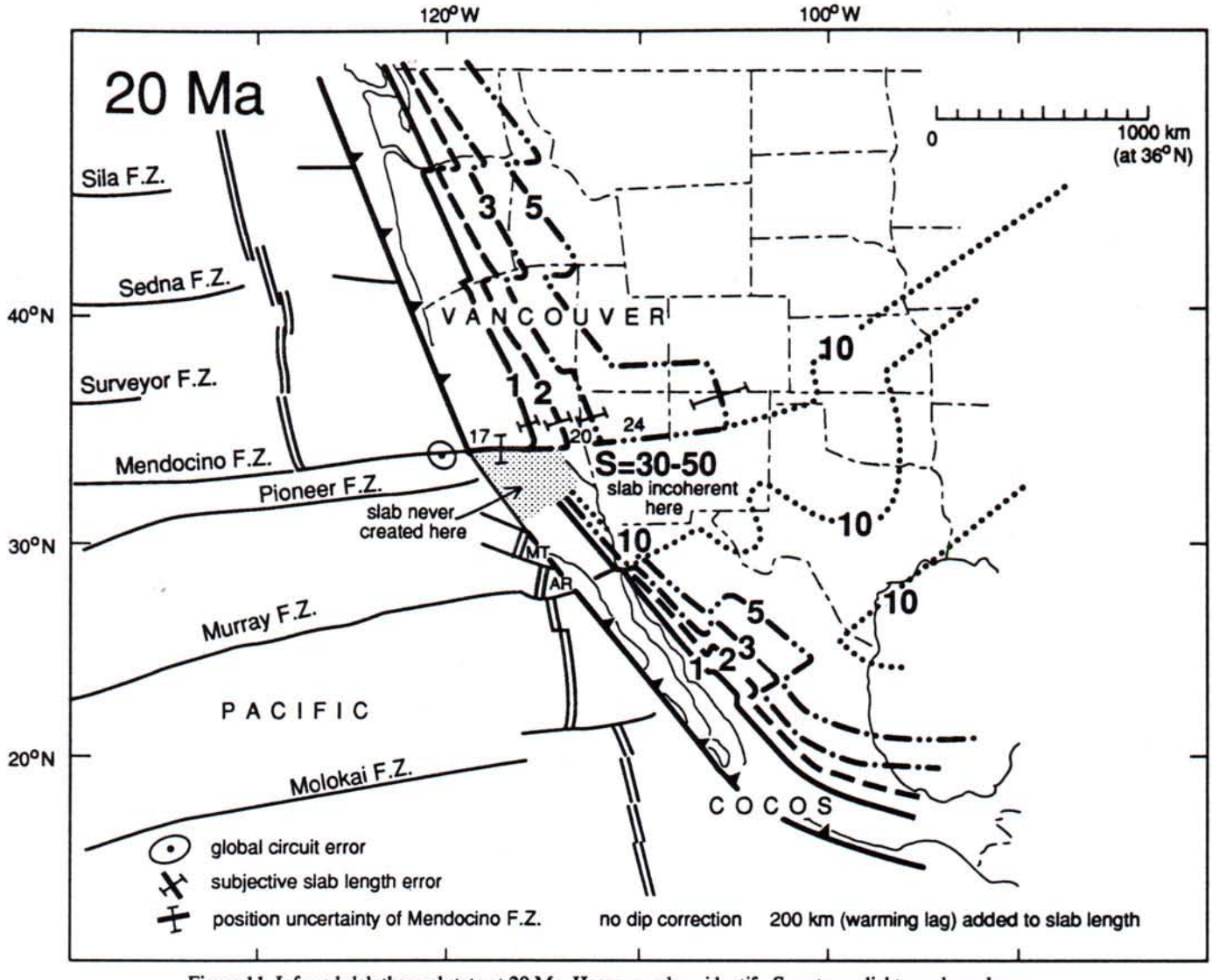

Figure 11. Inferred slab thermal state at 20 Ma. Heavy numbers identify S contours; light numbers show age on entry (Ma). In the Mendocino-Murray corridor, the MT and AR slabs are extremely short, and to their north no slab was ever formed (the slab window concept). The entire region of slab to the east of the emerging slab-free region has been subducted 30 to 50 times longer than necessary to become aseismic; i.e., it is probably indistinguishable from the asthenosphere.

occurred, asthenosphere would have upwelled to fill the break in the separating slab, with the possible consequence of voluminous, "dry," basaltic volcanism. In contrast, if the entire slab slowed, as described above, such a pulse of volcanism would not be expected.

20-Ma Reconstruction

By 20 Ma (Fig. 11), the slab just south of the subducted Mendocino fracture zone would have been subducted 30 to 50 times longer than necessary to become aseismic, and therefore we infer that it was indistinguishable from asthenosphere. Note that to the north of the subducted Mendocino fracture zone the slab persisted, whereas to the south it was gone. This slab–no slab edge coincides with the northern edge of Dickinson and Snyder's (1979a) proposed slab window, but it extends indefinitely to the east.

10-Ma and present-day reconstructions

The East Pacific Rise stopped spreading offshore of a large part of Baja California about 12 Ma, significantly lengthening the Pacific–North America boundary, as seen in the 10-Ma reconstruction (Fig. 12). We assume that subduction of this plate segment also stopped at this time. S values in Figure 13 were calculated assuming that the slab stopped moving but continued

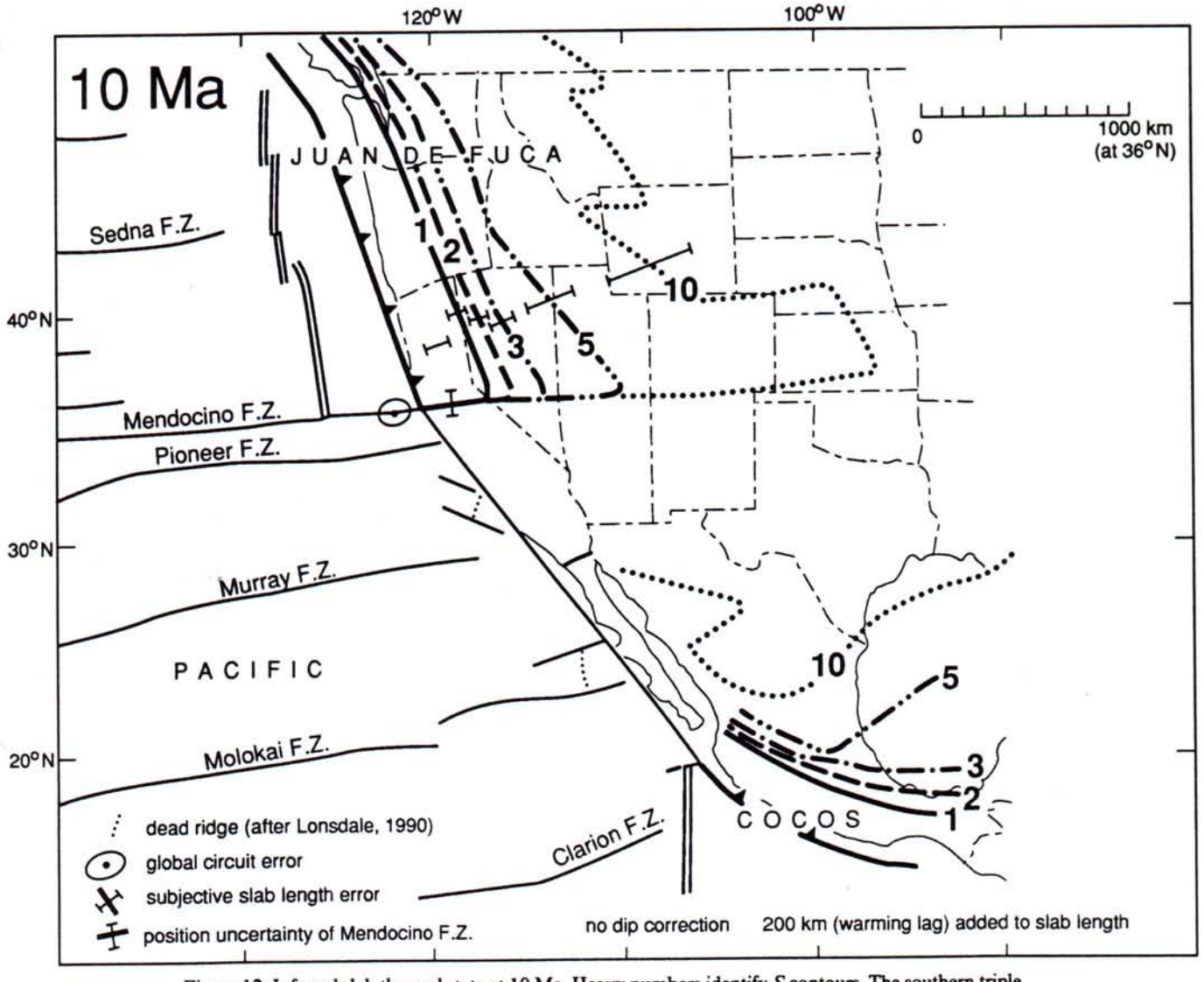

Figure 12. Inferred slab thermal state at 10 Ma. Heavy numbers identify S contours. The southern triple junction jumped south at 12 Ma, shutting off subduction along most of Baja California. Cocos slab beneath this section is assumed to have broken free of the main Cocos plate to the south and hence is positioned arbitrarily, but S values are so high that its location is not important.

to warm in situ. We include them merely to emphasize the extremely high S values that developed in the eastern and southern margins of the idealized "slab window"; the position of the slab is a moot point because it probably did not exist.

DISCUSSION

Figure 14 shows our interpretation of the approximate geometry of the slabs as the East Pacific Rise approached the trench off North America during the Cenozoic. For this figure, we how the $S = 2$ contour as the end of the slab, but we could equally well choose $S = 3$, shown dashed. With the addition of slab dip, these positions might correspond more closely to $S = 3$–5. In Figure 15, we summarize the evolution of slab geometry during the Cenozoic in a single picture, to emphasize changes through time.

A distinction needs to be made between the slab window concept, which describes a region where a slab was never formed, and the slab gap as described in this chapter, which includes regions of no slab originating both from nonformation and from thermal equilibration with the asthenosphere. A slab is not formed when spreading between two lithospheric plates occurs beneath a third plate rather than beneath water. It is the differing thermal character of the overlying medium—cold water versus a lithospheric plate—that distinguishes normal sea-floor spreading

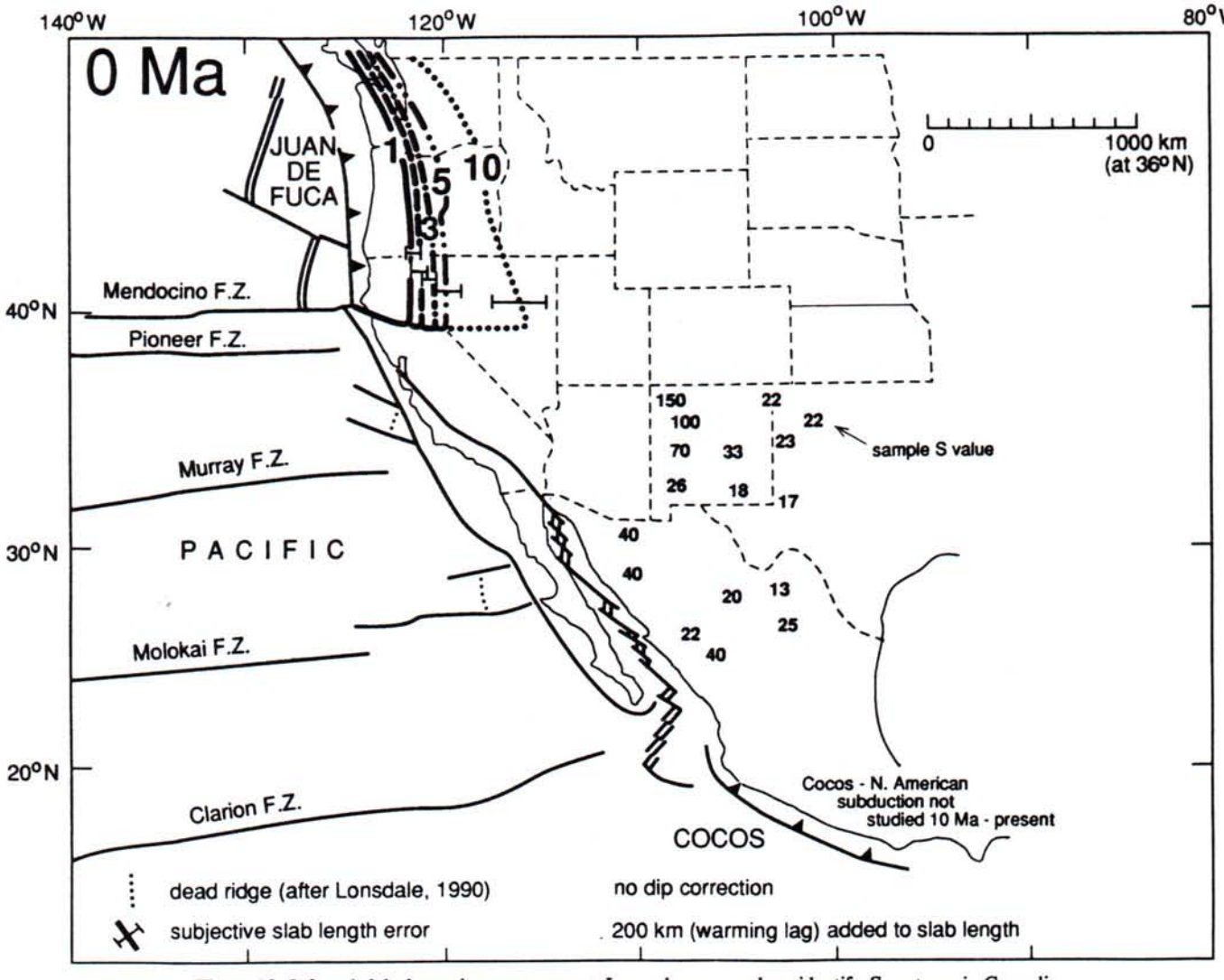

Figure 13. Inferred slab thermal state at present. Large, heavy numbers identify *S* contours in Cascadia (Juan de Fuca) slab. Smaller numbers are representative *S* values, not contoured. Position of slab with these values is arbitrary; values shown only to emphasize the extreme nature of the thermal parameters. Note small predicted size of Cascadia slab, consistent with observations that this slab lacks a well-developed Wadati-Benioff zone.

from formation of a slab window. Thus, the slab window does not include areas where a slab was overlain by water even for a short time before being subducted.

The thermal state of a very young slab is not very different from that of a slab window. In one important respect, however, the slab is different: no matter how young, it will be topped by hydrothermally altered basalts and thus will be capable of delivering water to the asthenosphere where it may induce arc volcanism (A. F. Glazner, written communication, 1988). This fact bears on the question of when arc volcanism would be expected to cease as subduction slows and stops.

As segments of the East Pacific rise arrived at the rim of North America, triple junctions were established at the two ends of the Pacific–North America plate boundary (San Andreas system) and moved apart as that boundary grew in length. The passage of these triple junctions should mark the cessation of subduction and arc magmatism, leaving a migrating "arc switch-off" in the geologic record (Christiansen and Lipman, 1972; Dickinson and Snyder, 1979a).

This is a good model for the northern, Mendocino triple junction since it corresponds to a straight, strong slab edge with a large thermal contrast and a true asthenospheric window edge. The southern triple junction, on the other hand, corresponds to a ragged, broken edge with vanishingly small thermal contrast and includes slowly subducting pieces and stalled slab fragments. Furthermore, because of uncertainties in the reconstructions of the plate positions and of the deformation of North America, the timing and position of the final cessation of subduction at the

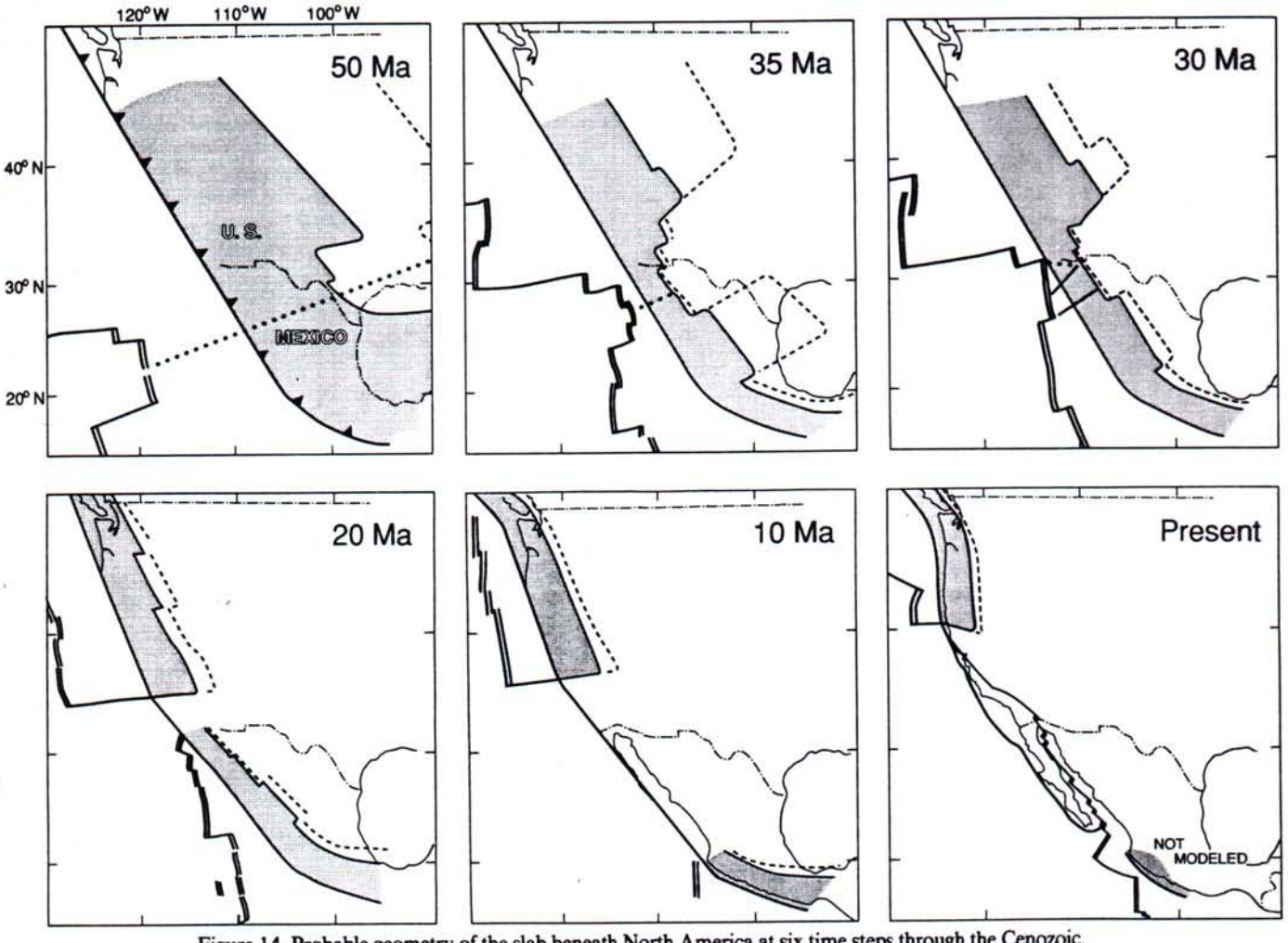

Figure 14. Probable geometry of the slab beneath North America at six time steps through the Cenozoic. Slab area with S value less than 2 is stippled. S = 3 contours shown dashed. Dotted lines show approximate locations of diffuse Vancouver-Farallon plate boundary. Note that the Laramide slab was relatively long. It shortened dramatically throughout the Cenozoic as the East Pacific Rise approached the trench. The development of a San Andreas transform was anticipated by and accompanied by a widening "slab gap." The transition, during the Paleogene, from a long cool slab to a short warm one happened rather quickly, suggesting that the long, flat slab may have disintegrated and fallen away in pieces.

southern triple junction are poorly known. The age of the youngest Pacific plate sea floor offshore gives us an upper bound for this switch-off age (Atwater, 1970, 1989), but we cannot preclude later slow subduction. California may have "overridden" the Pacific Plate by some unknown amount, covering up the anomalies that would give the true switch-off age.

We conclude that the position of the southern arc switch-off through time is poorly constrained by plate kinematic models. We hope, rather, that it will be established from the careful characterization and dating of continental magmatic rocks and that these may, in turn, help us determine the plate histories and interactions.

Note that the northern edge of the slab-free region is the only edge with a large thermal contrast, owing to the age difference across the Mendocino fracture zone (Figs. 10 through 13). We believe that this edge is the only well-defined edge of the slab gap and may be the only edge that has had observable geologic consequences for the North American continent. Thus our findings support postulated relations between the passage of this northern edge and geologic events such as a migrating arc switch-off (e.g., Snyder and others, 1976; Cross and Pilger, 1978; Glazner and Supplee, 1982), the uplift of the Colorado plateau and Sierra Nevada (Crough and Thompson, 1977), and, perhaps, the onset of major extensional episodes in the southern Basin and Range (e.g., Dickinson, 1981). In the California coast ranges, uplift patterns, lithosphere structure, and heat flow anomalies can likewise be attributed to this thermal edge and its migration (e.g., Lachenbruch and Sass, 1980; Zandt and Furlong, 1982).

CONCLUSIONS

The shrinkage of the slab beneath western North America during the Cenozoic is a predictable consequence of the approach of the ridge to the trench. We have roughly quantified the shape and thermal condition of the waning slabs by constructing contour maps of the thermal condition of the slab core, shown in some detail in Figures 8 through 13 and in summary in Figures 14 and 15. The positions of the particular thermal contours on our maps are quite uncertain. We believe that their primary value lies in their relative positions in space and their striking order-of-magnitude changes through time. Our conclusions, below, are all based on variations that are much greater than any that could be caused by the uncertainties.

During the time of the Laramide orogeny the slab was relatively long and cold, so the hypothesis that a flat slab extended intact as far inland as Colorado seems viable. Indeed, if the slab was flat or shallow dipping, it would have been even longer than shown on Figures 8, 14, and 15 because of our underestimate of the lag time arising from extended contact with the overriding plate.

During the mid-Cenozoic, the length of cold slab shortened significantly and rapidly everywhere. This is caused by a combination of decreasing age upon entry and a slowing in the subduction rate. If the early Cenozoic flat-slab scenario is adopted, this shortening of the slab is probably related to the mid-Cenozoic westward sweep of magmatism reported in many areas. Two small plates called the Monterey and Arguello plates broke free of the Farallon plate at 30 Ma, slowed, and underwent a clockwise change in spreading direction, indicating that the slab must have broken at this time.

If the idealized "slab window" hypothesis were correct, the slab that would have formed the eastern flank of this region was roughly 1 to 5 m.y. old when it was subducted, meaning that by 20 Ma, it would have been subducted 30 to 50 times longer than necessary to become aseismic (S = 30 to 50). We conclude that slab in this thermal state is indistinguishable from the asthenosphere. At 10 Ma and at present, the eastern flank is even hotter (S = 70 to 150). Thus, we conclude that the proposed slab window is better described as a "slab gap," a region of no slab flanked by coherent slabs to the north and south.

The slab gap developed gradually through the early and mid-Cenozoic, centered beneath northern Mexico. The gap first developed from the east, as a marked shortening in this portion of the slab. Subduction continued at the coast but with a disrupted and increasingly short-lived slab. Starting at 30 Ma, this short slab fragmented, and part of the slab gap began to be a region where slab was never formed (the "window" concept). The north-south widening of the slab gap continued to the present in concert with the evolution of the San Andreas transform regime on the North American margin. During the evolution of the gap, the entire pattern was drifting northwestward, as well, beneath North America.

The position and timing of the south-migrating edge of the slab gap throughout much of its history is indeterminate because of an ambiguity in the timing of cessation of subduction. The northern edge of the slab gap, defined by the Mendocino fracture zone, is probably the only margin of the no-slab region that may have had observable geologic consequences that can be related to the kinematically predicted position of the slab edge through time.

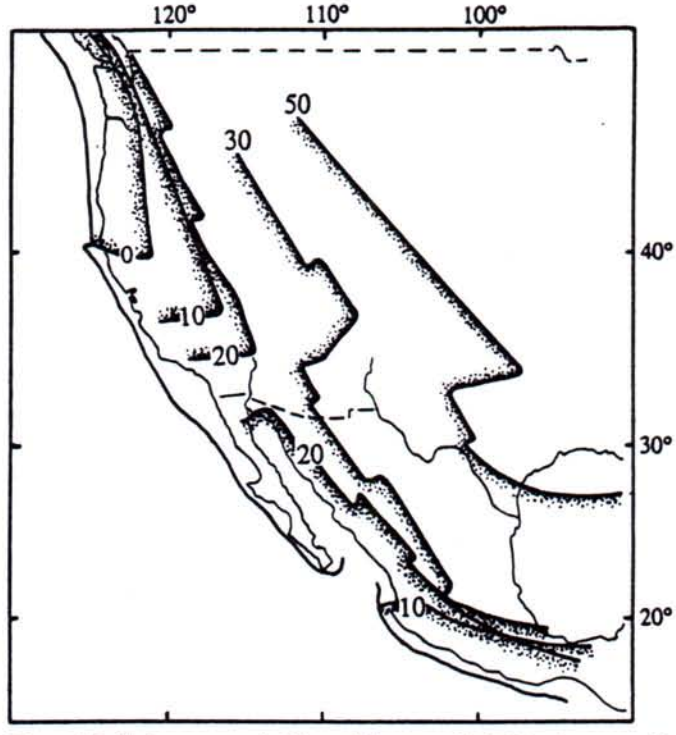

Figure 15. Slab geometry in Figure 14 summarized. Numbers are millions of years before present.

ACKNOWLEDGMENTS

We thank Joann Stock and Peter Molnar for providing global circuit data before publication, Peter Lonsdale for providing tectonic interpretations of offshore California and Baja California before publication, and Douglas Wilson for providing data on northeast Pacific fracture zones before publication. We thank Chris Scotese, Cathy Mayes, Lisa Gahagan, Larry Lawver, and John Sclater of the Paleo-Oceanographic Mapping Project at the University of Texas in Austin for helping us to digitize our magnetic anomaly interpretations and providing use of the Evans and Sutherland graphics computer. Cathy Mayes and Lisa Gahagan deserve special recognition for their generous assistance in making the reconstructions. David Crouch helped produce the figures. Partial funding for this project was provided by a University of California Academic Senate Research Grant. The paper benefited greatly from reviews by Joann Stock, Douglas Wilson, Suzanne Carbotte, and an anonymous reviewer.

APPENDIX 1: THEORETICAL CALCULATIONS OF THE THERMAL STATE OF THE SLAB

We have displayed the thermal state of subducting slabs by mapping contours of S and have noted that $S = 1$ corresponds approximately to the location of the seismic cutoff in modern slabs. We here explore the relationship between S and temperatures in the core of the slab.

McKenzie (1969, 1970) derived an equation for the potential temperature within a subducting slab (potential temperature is the temperature rock would have if raised to the surface). He assumed that the slab began with a thickness, h, and a constant potential temperature gradient from the temperature of seawater, $\theta = 273°K$ (0°C), at the top of the slab to that of the asthenosphere, $\theta = \theta_a$, at the bottom. Upon subduction, the slab is bathed in asthenosphere at $\theta = \theta_a$. It warms up by heat flowing in through both surfaces.

Using the coordinate system shown in Figure A1, the equation for potential temperature (in °K), modified from McKenzie (1970), is

$$\theta(x,z) = \theta_a + 2(\theta_a - 273)\sum_{n=1}^{\infty}\frac{(-1)^n}{n\pi}\exp\left[\frac{Rx}{h}\left(1-\sqrt{1+\frac{n^2\pi^2}{R^2}}\right)\right]\sin\frac{n\pi z}{h} \qquad (1)$$

where R is the thermal Reynolds number, $R \equiv \frac{\rho C_p v h}{2k}$, and θ_a is the potential temperature of the asthenosphere, $\theta_a \sim 1473°K$, or 1200°C, and where h is the slab thickness in cm, v is the subduction speed in cm/sec, ρ is the density, $\rho \sim 3.35$ g/cm^3, C_p is the heat capacity, $C_p \sim 10^7$ erg/(g°C), and k is the thermal conductivity, $k \sim 3 \times 10^5$ erg/(cm°C sec).

Some of these parameters, in turn, can be combined as K, the thermal diffusivity.

$$K = \frac{k}{\rho C_p}, \quad K \sim 9 \times 10^{-3}\ \text{cm}^2/\text{sec} \qquad (2)$$

and

$$R = \frac{vh}{2K}. \qquad (3)$$

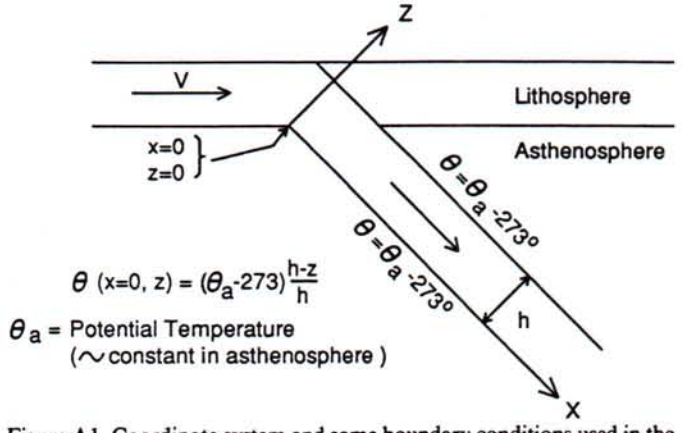

Figure A1. Coordinate system and some boundary conditions used in the calculation of the thermal state of a subducting slab, modified from McKenzie (1970).

The square root term in the exponential in equation (1) can be expressed as a binomial series, and since $R >> \pi$, we keep only the first two terms.

Substituting these and equation (3) into equation (1), we get

$$\theta(x,z) = \theta_a + 2(\theta_a - 273)\sum_{n=1}^{\infty}\frac{(-1)^n}{n\pi}\exp\left[-\frac{n^2\pi^2 Kx}{vh^2}\right]\sin\frac{n\pi z}{h}. \qquad (4)$$

We would like to explore this expression in relation to our parameter S, in which

$$S = \frac{\text{time since subduction} \times 10}{\text{age upon subduction}}$$

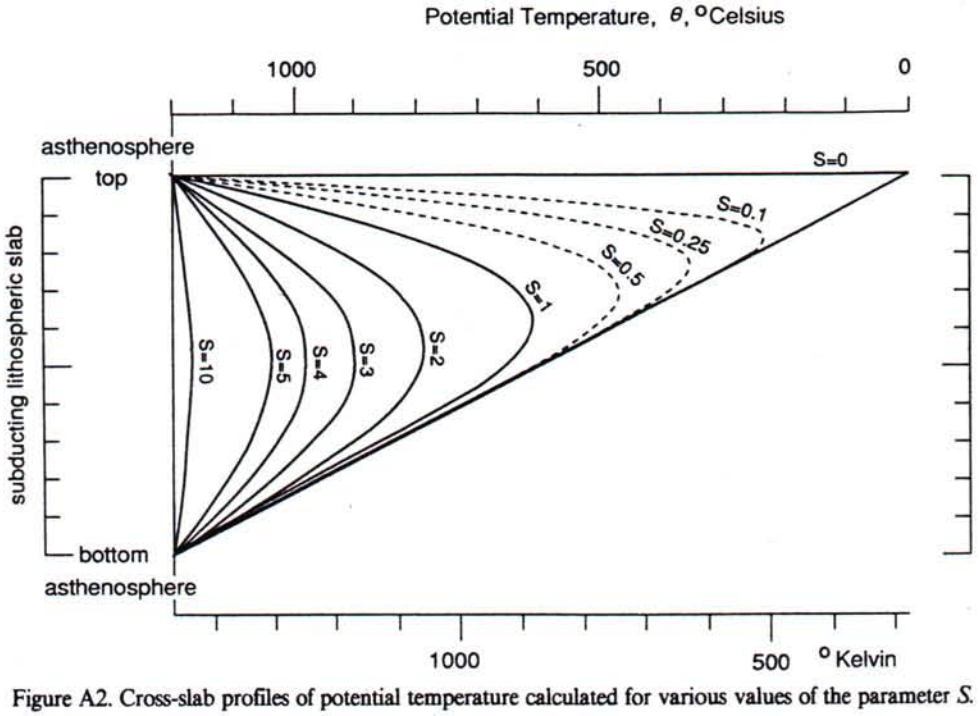

Figure A2. Cross-slab profiles of potential temperature calculated for various values of the parameter S.

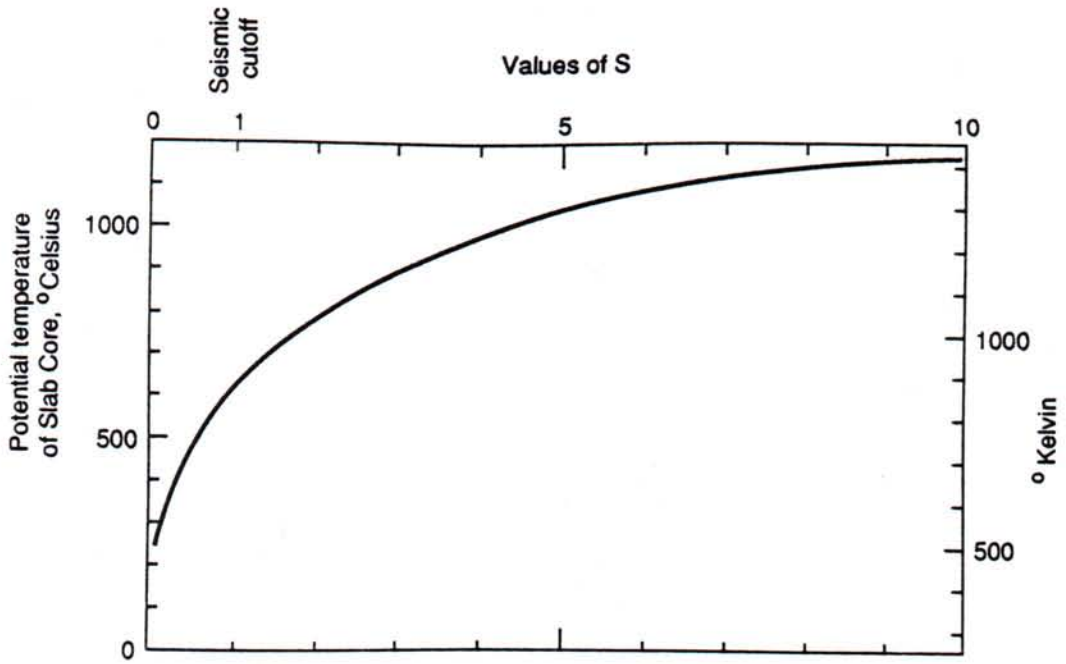

Figure A3. Minimum potential temperature in the slab versus S value.

The thickness of an oceanic plate, h, has been shown to be approximately proportional to the square root of its age, or $h(\text{km}) = 9.4t^{1/2}$ (m.y.) for plates less than about 100 m.y. old (Parker and Oldenburg, 1973; Parsons and Sclater, 1977), or $t(\text{sec}) = 35.65h^2$ (cm).

For a constant subduction velocity, the time since subduction is equal to x/v. Thus,

$$S = \frac{x}{Cvh^2} \tag{5}$$

where $C = 3.56$. Note that for a constant plate age and subduction velocity, S is simply proportional to distance down slab.

Substituting (5) in (4), we have:

$$\theta(x,z) = \theta_a + 2(\theta_a - 273)\sum_{n=1}^{\infty} \frac{(-1)^n}{n\pi} \exp\left[-Cn^2\pi^2 KS\right] \sin\frac{n\pi z}{h} \tag{6}$$

Figure A2 presents cross-slab profiles of potential temperature calculated from equation (6) at points down the slab corresponding to various values of S. The slab was assumed to start out with the temperature profile labeled $S = 0$. The calculated curves show that the cold top of the slab heats quickly at first as heat flows across the steep thermal gradient there. By the time the slab has been subducted for the duration corresponding to $S = 1$, the coldest core of the slab is found well below the top surface and has heated to more than half of θ_a, the asthenosphere potential temperature. Heating during subsequent steps is much slower because of the reduced gradients.

Figure A3 shows minimum potential temperature, i.e., the potential temperature of the cold core of the slab, for increasing values of S. For our purposes, we would like to know the value of S at which the slab becomes so hot that it is too weak to continue to act as a rigid plate. We do not know at what temperature this slab failure will occur, but we note that by the time the slab has reached $S = 3$, its coldest core has reached 77 percent of θ_a. At $S = 6$, its core is 90 percent of θ_a, and it is practically indistinguishable from the asthenosphere.

REFERENCES CITED

Atwater, T. M., 1970, Implications of plate tectonics for the Cenozoic tectonic evolution of western North America: Geological Society of America Bulletin, v. 81, p. 3518–3536.

—— , 1989, Plate tectonic history of the northeast Pacific and western North America, *in* Winterer, E. L., Hussong, D. M., and Decker, R. W., eds., The Eastern Pacific Ocean and Hawaii: Boulder, Colorado, Geological Society of America, The Geology of North America, v. N, p. 21–72.

Atwater, T. M., and Severinghaus, J., 1987, Propagating rifts, overlapping spreading centers, and duelling propagators in the northeast Pacific magnetic anomaly record: EOS Transactions of the American Geophysical Union, v. 68, p. 1493.

—— , 1989, Tectonic maps of the northeast Pacific, *in* Winterer, E. L., Hussong, D. M., and Decker, R. W., eds., The Eastern Pacific Ocean and Hawaii: Boulder, Colorado, Geological Society of America, The Geology of North America, v. N, p. 15–20.

Berggren, W. A., Kent, D. V., Flynn, J. J., and van Couvering, J. A., 1985, Cenozoic geochronology: Geological Society of America Bulletin, v. 96, p. 1407–1418.

Bird, P., 1984, Laramide crustal thickening event in the Rocky mountain foreland and Great Plains: Tectonics, v. 3, p. 741–758.

—— , 1988, Formation of the Rocky Mountains, western United States; A continuum computer model: Science, v. 239, p. 1501–1507.

Boyd, T. A., and Creager, K. C., 1987, Kinematic flow model of the Aleutian Slab: EOS Transactions of the American Geophysical Union, v. 68, p. 1500.

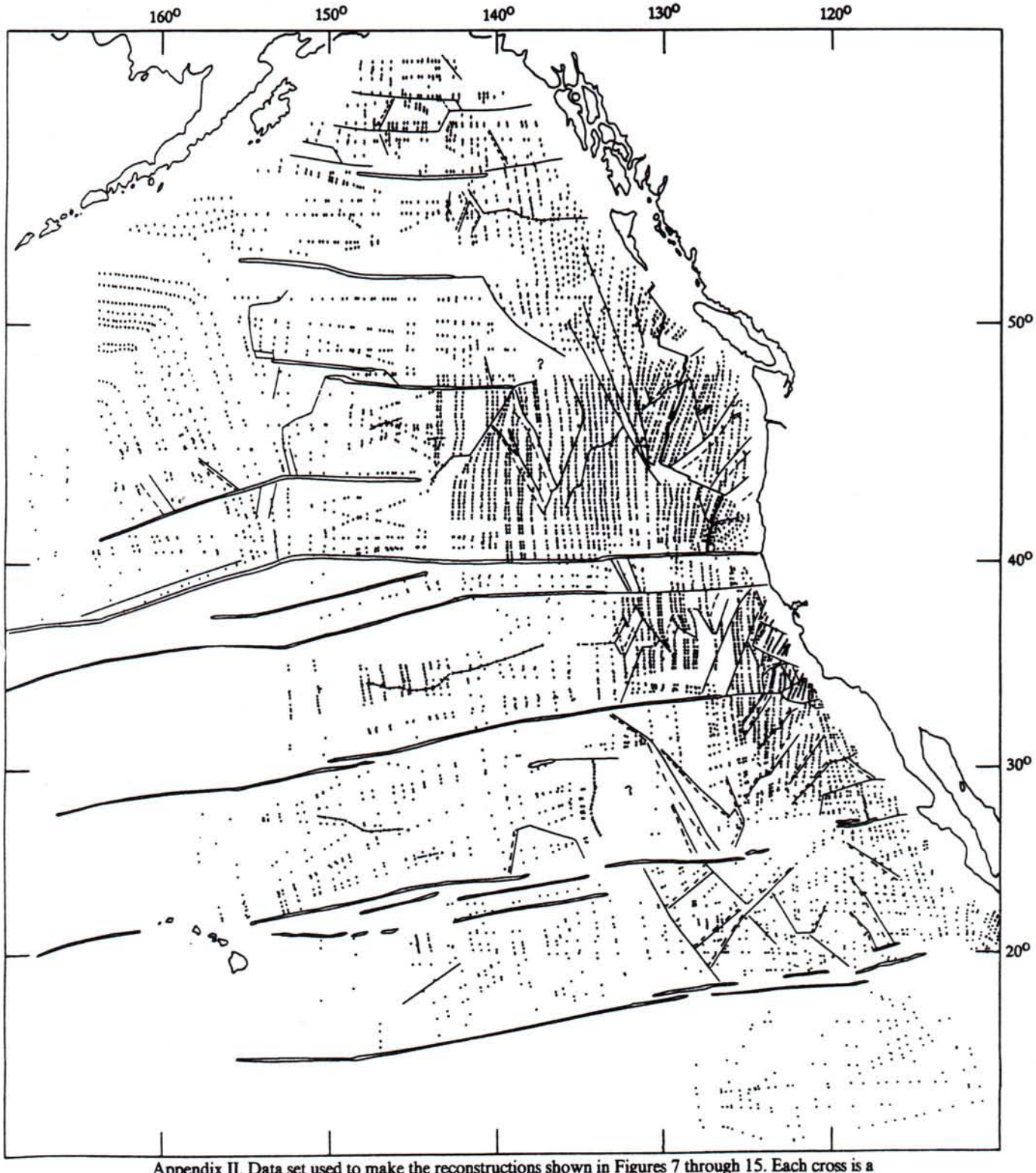

Appendix II. Data set used to make the reconstructions shown in Figures 7 through 15. Each cross is a data point representing a ship crossing of a magnetic anomaly. Available in digital form from the Paleo-Oceanographic Mapping Project, Institute for Geophysics, University of Texas at Austin.

Chen, W. P., and Molnar, P., 1983, Focal depths of intracontinental and intraplate earthquakes and their implications for the thermal and mechanical properties of the lithosphere: Journal of Geophysical Research, v. 88, p. 4183–4214.

Christiansen, R. L., and Lipman, P. W., 1972, Cenozoic volcanism and plate tectonic evolution of the western United States; Part 2, Late Cenozoic: Proceedings of the Royal Society of London, v. 271, p. 249–284.

Coney, P. J., and Reynolds, S. J., 1977, Cordilleran Benioff zones: Nature, v. 270, p. 403–406.

Creager, K. C., and Jordan, T. H., 1986, Slab penetration into the lower mantle beneath the Mariana and other island arcs of the northwest Pacific: Journal of Geophysical Research, v. 91, p. 3573–3589.

Cross, T. A., 1986, Tectonic controls of foreland basin subsidence and Laramide style deformation, western United States: International Association of Sedimentologists Special Publication 8, p. 15–39.

Cross, T. A., and Pilger, R. H., Jr., 1978, Constraints on absolute motion and plate interaction inferred from Cenozoic igneous activity in the western United States: American Journal of Science, v. 278, p. 865–902.

Crough, T. S., and Thompson, G. A., 1977, Upper mantle origin of Sierra Nevada uplift: Geology, v. 5, p. 396–399.

Dickinson, W. R., 1981, Plate tectonic evolution of the southern Cordillera, *in* Dickinson, W. R., and Payne, W. D., eds., Relations of tectonics to ore bodies in the southern Cordillera: Arizona Geological Society Digest, v. 14, p. 113–135.

Dickinson, W. R., and Snyder, W. S., 1979a, Geometry of subducted slabs related to San Andreas Transform: Journal of Geology, v. 87, p. 609–627.

—— , 1979b, Geometry of triple junctions related to San Andreas transform: Journal of Geophysical Research, v. 84, p. 561–572.

Frei, L. S., 1986, Additional paleomagnetic results from the Sierra Nevada; Further constraints on Basin and Range extension and northward displacement in the western United States: Geological Society of America Bulletin, v. 97, p. 840–849.

Glazner, A. F., and Supplee, J. A., 1982, Migration of Tertiary volcanism in the southwestern United States and subduction of the Mendocino fracture zone: Earth and Planetary Science Letters, v. 60, p. 429–436.

Goetze, C., 1978, The mechanism of creep in olivine: Philosophical Transactions of the Royal Society of London, series A, v. 288, p. 99–119.

Hager, B. H., 1986, The layered mantle; To be or not to be? Yes!: EOS Transactions of the American Geophysical Union, v. 67, p. 1257.

Hyndman, R. D., Riddihough, R. P., and Herzer, R., 1979, The Nootka Fault Zone; A new plate boundary off western Canada: Geophysical Journal of the Royal Astronomical Society of London, v. 58, p. 667–683.

Jarrard, R. D., 1986, Relations among subduction parameters: Reviews of Geophysics, v. 24, p. 217–284.

Kent, D. V., and Gradstein, F. M., 1985, A Cretaceous and Jurassic geochronology: Geological Society of America Bulletin, v. 96, p. 1419–1427.

Lachenbruch, A. H., and Sass, J. H., 1980, Flow and energetics of the San Andreas fault zone: Journal of Geophysical Research, v. 85, p. 6185–6223.

Lonsdale, P., 1990, Structural patterns of the Pacific floor offshore of Peninsular California, *in* Dauphin, J., ed., Gulf and Peninsula Provinces of the Californias: American Association of Petroleum Geologists Memoir 47 (in press).

McKenzie, D. P., 1969, Speculations on the consequences and causes of plate motions: Geophysical Journal of the Royal Astronomical Society of London, v. 18, p. 1–32.

—— , 1970, Temperature and potential temperature beneath island arcs: Tectonophysics, v. 10, p. 357–366.

Menard, H. W., 1978, Fragmentation of the Farallon plate by pivoting subduction: Journal of Geology, v. 86, p. 99–110.

Michaelson, C. A. and Weaver, C. S., 1986, Upper mantle structure from teleseismic P wave arrivals in Washington and northern Oregon: Journal of Geophysical Research, v. 91, p. 2077–2094.

Molnar, P., Freedman, D., and Shih, J.S.F., 1979, Lengths of intermediate and deep seismic zones and temperatures in downgoing slabs of lithosphere: Geophysical Journal of the Royal Astronomical Society of London, v. 56, p. 41–54.

Parker, R. L., and Oldenburg, D. W., 1973, Thermal models of ocean ridges: Nature Physical Science, v. 242, p. 137–139.

Parsons, B., and McKenzie, D., 1978, Mantle convection and the thermal structure of the plates: Journal of Geophysical Research, v. 83, p. 4485–4496.

Parsons, B., and Sclater, J. G., 1977, An analysis of the variation of ocean floor bathymetry and heat flow with age: Journal of Geophysical Research, v. 82, p. 803–827.

Pennington, W. D., 1983, Role of shallow phase changes in the subduction of oceanic crust: Science, v. 220, p. 1045–1047.

Rasmussen, J. R., Humphreys, E., and Dueker, K. G., 1987, P-wave velocity structure of the upper mantle beneath Washington and northern Oregon: EOS Transactions of the American Geophysical Union, v. 68, p. 1379.

Ringwood, A. E., and Green, D. H., 1966, An experimental investigation of the gabbro-eclogite transformation and some geophysical implications: Tectonophysics, v. 3, p. 383–427.

Rosa, J.W.C., and Molnar, P., 1988, Uncertainties in reconstructions of the Pacific, Farallon, Vancouver, and Kula plates and constraints on the rigidity of the Pacific and Farallon (and Vancouver) plates between 72 and 35 Ma: Journal of Geophysical Research, v. 93, p. 2997–3008.

Snyder, W. S., Dickinson, W. R., and Silberman, M. L., 1976, Tectonic implications of space-time patterns of Cenozoic magmatism in the western United States: Earth and Planetary Science Letters, v. 32, p. 91–106.

Stock, J., and Molnar, P., 1988, Uncertainties and implications of the Late Cretaceous and Tertiary position of North America relative to the Farallon, Kula, and Pacific plates: Tectonics, v. 7, p. 1339–1384.

Sugi, N., and Uyeda, S., 1984, Subduction of young oceanic plates: Bulletin de la Société de France, v. 26, p. 245–254.

Theberge, A. E., Jr., 1971, Magnetic survey off southern California and Baja California: Rockwell, Maryland, National Oceanic and Atmospheric Administration Marine Geophysics Group Operational Data Report NOS DR-12, 10 p.

Weaver, C. S. and Baker, G. E., 1988, Geometry of the Juan de Fuca plate beneath Washington and northern Oregon from seismicity: Bulletin of the Seismological Society of America, v. 78, p. 264–275.

Wernicke, B. P., Axen, G. J., and Snow, J. K., 1988, Basin and Range extensional tectonics at the latitude of Las Vegas, Nevada: Geological Society of America Bulletin, v. 100, p. 1738–1757.

Wilson, D. S., 1988, Tectonic history of the Juan de Fuca Ridge over the last 40 million years: Journal of Geophysical Research, v. 93, p. 11863–11876.

Wortel, R., 1982, Seismicity and rheology of subducted slabs: Nature, v. 296, p. 553–556.

Zandt, G., and Furlong, K. P., 1982, Evolution and thickness of the lithosphere beneath coastal California: Geology, v. 10, p. 376–381.

MANUSCRIPT ACCEPTED BY THE SOCIETY AUGUST 21, 1989

Printed in U.S.A.